Baseline morphometry of the pterygoid hamulus in a neonatal South African population

A thesis submitted to the Department of Anatomy, School of Medicine, Faculty of Health Sciences, University of Pretoria, in fulfilment of the requirements for the degree of MSc in Clinical Anatomy

Pretoria 2020

Candidate:
Ms. Helene Biemond
14021758

Supervisors:
Dr. G. Roode [1]
Prof. A van Schoor[1]

Head of Department:
Prof P. Soma[1]

[1] University of Pretoria, Faculty of Health Sciences, Department of Anatomy

UNIVERSITY OF PRETORIA

Declaration

Title: Baseline morphometry of the pterygoid hamulus in a neonatal South African population

I, ***Helene Biemond,*** student number ***14021758,*** understand what plagiarism is and am aware of the University's policy in this regard. I declare that this thesis is my own original work. Where other people's work has been used (either from a printed source, internet or any other source), this has been properly acknowledged and referenced in accordance with departmental requirements. I have not used work previously produced by another student or any other person to hand in as my own. I have not allowed, and will not allow, anyone to copy my work with the intention of passing it off as his or her own work. This thesis is being submitted for the degree of MSc in Anatomy at the University of Pretoria. It has not been submitted before for any other degree or examination at this or any other Institution.

This, the 25th day of March 2020

TABLE OF CONTENTS

List of Figures V
List of Tables VII
List of Abbreviations IX
Anatomical abbreviations IX
Measurement abbreviation IX
Statistical abbreviations IX
Acknowledgements XI
Executive Summary XII
1. Introduction 1
2. Literature review 3
2.1 Anatomy 3
2.1.1 Pterygoid hamulus 3
2.1.2 Hard palate 4
2.1.3 Surrounding musculature 4
2.2 Pathology 6
2.3 Similar studies 9
2.4 Corrective procedure: Tensor sling procedure 13
3. Aim 16
3.1 Research objectives 16
4. Materials and methods 17
4.1 Setting 17
4.2 Study design 17
4.3 Sample size 17
4.4 Procedure for CBCT scanning 17
4.5 Quantitative data measurements 19
4.6 Statistical analysis 25
4.7 Ethical considerations 27
5. Results 28
5.1 Test for normality 28
5.2 Comparative tests 30
5.3 Correlation tests 32
5.4 Regression analysis 33

5.5 Difference in weight **33**
5.6 Difference in population groups **38**
5.7 Different frequencies of angles observed **41**
5.8 Intra-observer error **43**
5.9 Inter-observer error **44**
6. Discussion **45**
6.1 Descriptive statistics **45**
6.2 Relationships between variables **45**
6.3 Comparing variables with weight populations **45**
6.4 Comparing variables with population groups **47**
6.5 Observations of frequencies of the angles of inclination **48**
6.6 Comparing results to other studies **49**
6.7 Abnormality found **51**
6.8 Limitations of the study **53**
7. Conclusion **54**
8. Future recommendations **56**
8. References **57**
9. Appendices **59**
9.1 Appendix A **59**
9.2 Appendix B **66**
9.3 Appendix C **68**
9.4 Appendix D **69**
9.5 Appendix E **73**
9.6 Appendix F **76**

LIST OF FIGURES

Figure 2.1.1: Linear dimensions of the pterygoid hamulus according to Putz and Kroyer[13] **3**
Figure 2.2.1: An elongated hamulus in situ after exposure[4] **7**
Figure 2.2.2: The removed elongated tip of the pterygoid hamulus[4] **8**
Figure 2.2.3: Sutures indicating where the elongated hamuli were removed[4] **8**
Figure 2.4.1: A visual representation of the tensor sling procedure showing the route of placing the suturing material[23] **14**
Figure 4.4.1 Standardised position that the neonate is set within the CBCT machine **18**
Figure 4.5.1: CBCT scan of a neonatal cadaver, showing most of the sphenoid bone in the coronal plane on the section where the pterygoid hamulus was best observed **19**
Figure 4.5.2: Horizontal (axial) plane in the sagittal section running through the anterior nasal spine (ANS) and the posterior nasal spine (PNS) **20**
Figure 4.5.3: Enlarged CBCT scan in the coronal plane indicating the pterygoid hamuli **21**
Figure 4.5.4: Enlarged CBCT scan in the sagittal plane indicating the left pterygoid hamulus **22**
Figure 4.5.5: Enlarged CBCT scan in the axial plane indicating the pterygoid hamuli and the posterior nasal spine **23**
Figure 4.5.6: Enlarged CBCT scan in the coronal plane indicating the pterygoid hamuli **24**
Figure 4.5.7: Enlarged CBCT scan in the sagittal plane indicating the pterygoid hamulus **25**
Figure 6.7.1: CBCT scan in the coronal plane of a neonatal sphenoid indicating the pterygoid hamuli. The blue circles indicate the abnormality first observed in the coronal plane **51**
Figure 6.7.2: CBCT scan in the sagittal plane of a neonatal skull indicating the pterygoid hamulus. The blue circle indicates the elongated hamulus **52**
A.5: Regression formula between PNS and height for combined measurements **62**
A.6: Regression formula between IHD and height for combined measurements **63**
A.7: Regression formula between PNS and weight for combined measurements **63**

A.8: Regression formula between IHD and weight for combined measurements **64**
A.9: Regression formula between IHD and PNS for combined measurements **64**
B.3: Regression formula between the PNS and the IHD in the W0 sample **67**
B.4: Regression formula between the PNS and the IHD in the W1 sample **67**
C.2: Regression formula between the LH and the PNS of the WA population **68**
D.1: Visualisation of the Bland and Altman intra-observer error for LH (mm)..... **69**
D.2: Visualisation of the Bland and Altman intra-observer error for WHC (mm)..... **69**
D.3: Visualisation of the Bland and Altman intra-observer error for WHS (mm)..... **70**
D.4: Visualisation of the Bland and Altman intra-observer error for PNS (mm)..... **70**
D.5: Visualisation of the Bland and Altman intra-observer error for IC (degrees)..... **71**
D.6: Visualisation of the Bland and Altman intra-observer error for IS (degrees)..... **71**
D.7: Visualisation of the Bland and Altman intra-observer error for IHD (mm)..... **72**
E.1: Visualisation of the Bland and Altman inter-observer error for LH (mm)..... **73**
E.2: Visualisation of the Bland and Altman inter-observer error for WHC (mm)..... **73**
E.3: Visualisation of the Bland and Altman inter-observer error for PNS (mm)..... **74**
E.4: Visualisation of the Bland and Altman inter-observer error for IC (degrees)..... **74**
E.5: Visualisation of the Bland and Altman inter-observer error for IS (degrees)..... **75**
E.6: Visualisation of the Bland and Altman inter-observer error for IHD (mm)..... **75**

LIST OF TABLES

Table 4.3.1: Demographic details of the sample **17**
Table 5.1.1: Standardised descriptive statistical analysis after the removal of measurements corresponding to outlying Z-scores **29**
Table 5.1.2: Shapiro-Wilk test, Skewness and Kurtosis of standardised measurements, with p-values indicating measurements that could not be compared using a paired t-test highlighted (not normally distributed) **30**
Table 5.2.1: Paired t-test comparing the normally distributed right and left measurements, with p-values indicating that they could be combined **30**
Table 5.2.2: Wilcoxon Signed-Rank test comparing the left and right measurements that were not normally distributed, with p-values indicating that the measurements could be combined **31**
Table 5.2.3: Descriptive statistical analysis of combined left and right measurements **31**
Table 5.3.1: Correlation coefficient between notable correlation pairs for combined data **32**
Table 5.4.1: Regression analyses between correlation pairs for combined data **33**
Table 5.5.1: Frequency table indicating the frequency with which neonates were classified as W0 and W1 ..... **34**
Table 5.5.2: Levene's test for equality of variances, assessing the assumption of equal variance for the population W0 and W1, with p-values lower than 0.05 highlighted. **34**
Table 5.5.3: Independent sample t-test for equality of means for W0 and W1. P-value higher than 0.05 is highlighted **35**
Table 5.5.4: Descriptive statistical analysis for W0 ..... **36**
Table 5.5.5: Descriptive statistical analysis for W1 ..... **36**
Table 5.5.6: Regression analysis between the correlation pair for the W0 sample.. **37**
Table 5.5.7: Regression analysis between the correlation pair for the W1 sample.. **37**
Table 5.6.1: Frequency table indicating the frequency with which neonates were classified as WA and BB **38**
Table 5.6.2: Levene's test for equality of variances, assessing the assumption of equal variance between populations WA and BB, with p-values lower than 0.05 highlighted **39**

Table 5.6.3: Independent sample t-test for equality of means for WA and BB. P-value lower than 0.05 is highlighted **39**
Table 5.6.4: Descriptive statistical analysis for the LH measurement of WA and BB **40**
Table 5.6.5: Regression analysis between the correlation pair WA **40**
Table 5.7.1: Frequency of IS0 (angle ≤ 90°) and IS1 (angle > 90°) observed in the combined data group, the two groups separated by weight, and the two groups separated by their population group **42**
Table 5.7.2: Frequency of IC0 (angle ≤ 90°) and IC1 (angle > 90°) observed in the combined data group, the two groups separated by weight, and the two groups separated by their population group **42**
Table 5.8.1: Bland and Altman statistics comparison for intra-observer error, all measurements in mm and degrees **43**
Table 5.9.1: Bland and Altman statistics comparison for inter-observer error, all measurements in mm and degrees **44**
Table 6.6.1: Summary of all the quantitative measurements for all the studies related to the morphometry of the pterygoid hamulus **50**
A.1: Data collection sheet for measurements made, with all distances and lengths measured in millimetres and all angles measured in degrees. Outliers are highlighted **59**
A.2: Descriptive statistical analysis of all measurements before they were standardised, measured in millimetres **60**
A.3: Shapiro-Wilk test, Skewness and Kurtosis of unstandardised measurements . **61**
A.4: Pearson's correlation test indicating the strength of correlation between different measurements of combined left and right sides **61**
B.1: Pearson's correlation test indicating the strength of correlation between different measurements for W0 ..... **65**
B.2: Pearson's correlation test indicating the strength of correlation between different measurements for W1 ..... **65**
C.1: Pearson's correlation test indicating the strength of correlation between LH and the different measurements for the WA and BB populations **68**

LIST OF ABBREVIATIONS

Anatomical abbreviations

BMI: Body Mass Index, measured in kg/m^2

CBCT: Cone Beam Computed Tomography

ODH: Oral-and-Dental Hospital

Measurement abbreviations

IC: Inclination of the pterygoid hamulus in the coronal plane

IS: Inclination of the pterygoid hamulus in the sagittal plane

IHD: Inter-hamular distance

LH: Length of the pterygoid hamulus

PNS: Distance from the inferior tip of the pterygoid hamulus to the posterior nasal spine

WHC: Width of the pterygoid hamulus in the coronal plane

WHS: Width of the pterygoid hamulus in the sagittal plane

Statistical abbreviations

B: Slope of the line between the dependent variable and the independent variable

BB: Black population

CI: Confidence interval

df: degrees of freedom

F: Tests the null hypothesis that the variance is equal

IC0: Inclination in the coronal plane less or equal to 90°

IC1: Inclination in the coronal plane more than 90°

IS0: Inclination in the sagittal plane less or equal to 90°

IS1: Inclination in the sagittal plane more than 90°

Max: Maximum

Min: Minimum

N: Population size

P-value: Probability of obtaining observed result of test

r: Rho, Spearman's rank correlation coefficient

R^2: How close the data is to the fitted regression line

SD: Standard deviation

Std: Standard

t: The size of the difference relative to the variation in your sample data

WA: White population

W0: Population with weight less than or equal to 1kg

W1: Population with weight more than 1kg

Z: Measurement of a value's relationship to the mean

AKNOWLEDGEMENTS

I would like to thank my parents for their emotional and financial support over the course of my degree. Also the rest of my family for their support and understanding during hard decisions and hard times.

Thank you to all my friends for their support and sometime morbid curiosity about what I do. Thank you to Shavana Govender for all the annoying questions I asked when stuck on something. To Niel van Tonder, thank you for the help with the statistics, and continuously explaining the same things when I got confused.

A huge thank you to my supervisor Dr. Giel Roode for giving me the chance to work on such an amazing topic. Thank you for all the support and assistance during this process. Thank you especially for helping with the data collection - which was a bit of a challenging experience for a 24 year old - considering the age of the sample and the sheer amount of new-borns to be scanned. I would also like to thank Dr. Andre Uys for helping me with the CBCT machine and the data collection program.

Thank you to my co-supervisor Prof. Albert van Schoor for helping us out with this project, especially concerning the finer details I was ignorant on. Thank you for helping me when I decided at the 11th hour to do my masters.

To the Department of Anatomy, thank you all for being the best example of what a lecturer and researcher can be. Thank you for treating us with respect and patience. Thank you to the staff and students working in the Oral-and-Dental Hospital for allowing me to traipse about the premises and use the machine and computers.

EXECUTIVE SUMMARY

The pterygoid hamulus is a hook-like bony structure found at the inferior end of the medial pterygoid plate of the sphenoid bone. The pterygoid hamulus in adults has been a structure that, until recently, has not been fully described in the literature. However, today the anatomy is sufficiently described, but one omitted key point, is the anatomy in neonates.

In order to fully describe the structure in neonates, as opposed to the structure in adults, the method of measurement utilized in this study was set out by Orhan *et al*.[15] based on the anatomical landmarks described by Putz and Kroyer.[13] This further allowed this study to compare the results found with the results from previous studies. As this study is the first of its kind, it was a comparative study between the left and right sides, as well as population groups. This study was done on a neonatal population, with ages ranging from new-borns until the age of 28 days. This study was performed in order to fill this gap in knowledge where the neonatal pterygoid hamular anatomy in South Africa is concerned.

For neonates less than or equal to 1kg, the length of the pterygoid hamulus (LH) was 2.23±0.377mm, the width of the pterygoid hamulus in the coronal plane (WHC) was 0.938±0.162mm, the width of the pterygoid hamulus in the sagittal plane (WHS) was 1.68±0.373mm, the distance between the tip of the pterygoid hamulus and the posterior nasal spine (PNS) was 9.74±0.853mm, the inclination of the pterygoid hamulus in the coronal plane (IC) was 105±10.1°, the pterygoid inter-hamular distance (IHD) was 14.5±1.56mm.

For the neonates weighing more than 1 kg, the length of the pterygoid hamulus (LH) was 2.74±0.438mm, the width of the pterygoid hamulus in the coronal plane (WHC) was 1.12±0.226mm and the width of the pterygoid hamulus in the sagittal plane (WHS) was 1.87±0.446mm. The distance from the tip of the pterygoid hamulus to the posterior nasal spine (PNS) was 12.1±1.5mm. The inclination of the pterygoid hamulus in the coronal plane (IC) was 110±9.52°, and lastly, the pterygoid inter-hamular distance (IHD) was 18.5±2.72mm. For both weight classes, the inclination of the pterygoid hamulus in the sagittal plane (IS) was between 68.5° and 107.3°.

This study found that certain pterygoid hamulus morphometrics could be established from biometrics. The PNS and IHD measurements can be extrapolated from both height and weight. Furthermore the morphometrics IHD and PNS can be extrapolated from each other. There was no significant difference between sexes or population groups, or between left and right sides. Height and especially weight had an effect on measurements.

The South African morphometric database established in this study allows for a comparative evaluation of normal neonatal pterygoid hamular structure with that of the adult pterygoid hamulus and the pterygoid hamulus in cleft palate neonates. Demographics are not important where the pterygoid hamulus morphology is concerned but biometrics are, and need to be kept in mind by surgeons and researchers.

Keywords: new-born, Eustachian tube, cleft palate, elongated hamulus, tensor veli palatini, otitis media, tensor sling procedure.

1. Introduction

The pterygoid hamulus is a structure that was not accurately described in literature up until a few years ago. This investigator can only speculate as to why the structure was not thoroughly researched until recently, this might have been due to availability and cost of scanning equipment. This structure has now been researched and documented for adults, but there are still shortcomings related to neonates. The sources used in this study were obtained from studies performed on three different European populations and one on a Malaysian population. No study on a South African population could be found. As the ratios and types of population groups for European and Asian countries differ from those found in South Africa, the results found in these studies may not be applicable to South Africans, specifically the black South African population group.

The relation of the pterygoid hamulus to surrounding structures plays a role in various pathologies, such as cleft lip and palate, pterygoid hamulus syndrome as well as hamular bursitis and sleep apnoea and is important to consider in the planning of procedures to correct them.[1-5] The pterygoid hamulus is in close proximity to the pharynx, the tensor veli palatini muscle, the pterygopharyngeal part of the superior constrictor and the buccinator muscle. These muscles are responsible for or contribute to the separation of the nasal and oral cavities from each other, mainly by elevating the soft palate during swallowing. This important function may undergo change with deviation of normal pterygoid hamulus anatomy due to abnormalities or possibly corrective procedures.[6]

For example, a lengthened pterygoid hamulus, can have a negative impact on the surrounding structures and their functions.[7-9] A high incidence of middle ear infection has been observed in children that have undergone cleft palate reparative surgery. This high incidence of middle ear infection is due to the change in anatomy after the procedure regarding the Eustachian tube.[10-11]

Pathology of the pterygoid hamulus is difficult to diagnose due to the regional anatomy and embryological development of these structures. Furthermore, computed tomography (CT) and magnetic resonance imaging (MRI) scans can be very

expensive. This difficult diagnosis means that pain due to the pathology of the pterygoid hamulus is mostly misdiagnosed as conditions such as otitis media or trigeminal neuralgia due to the similar pain profile. Pterygoid hamular bursitis and elongation are two of the conditions that cause pain in the oropharyngeal and surrounding area.[12]

This project sought to give information on the pterygoid hamulus in a new light, separate from what can be found in the current literature, in order to help progress further studies where the hamulus plays a role in pathology or surgical reconstruction, as in new-born cleft palate patients.[13-16] By assembling this information in a comparative manner, we were able to provide a set of baseline parameters of the morphometry of the neonatal pterygoid hamulus, which until this point, is not available to maxillofacial and ear-nose and throat surgeons. This new set of data on the normal anatomy of this area allows evaluation of more comprehensive surgeries and new techniques.

Considering the fact that there are no studies of this kind that have been done on a neonatal South African population, including all population groups, this study focuses on this population niche thereby expanding the knowledge of the bone structure of South Africa's population. This is the largest study of its kind to date with a sample size of 74 neonates.

2. Literature review

2.1 Anatomy

2.1.1 Pterygoid hamulus

The pterygoid hamulus is described as a hook-like bony projection that curves laterally from the medial pterygoid plate, with a groove anteriorly for the tendon of the tensor veli palatini muscle.[6] According to Krmpotić- Nemanić *et al.*[14] this description of the structure of the pterygoid hamulus is only found in early infancy. They do not specify exactly when the anatomy changes.

As the pterygoid hamulus was rarely described in detail before 1999, further studies, such as those conducted by Putz and Kroyer,[13] Krmpotić- Nemanić *et al.,*[14] Orhan *et al.*[15] and Rajion *et al.*[16] have established a more comprehensive database of the pterygoid hamulus in European and Asian populations. Putz and Kroyer[13] were the first to give an exact description of the pterygoid hamulus, dividing it into the following linear dimensions; the base, the neck and a head (Figure 2.1.1). In contrast to the literature, they noted that the groove on the pterygoid hamulus was found on the lateral side of the pterygoid hamulus.

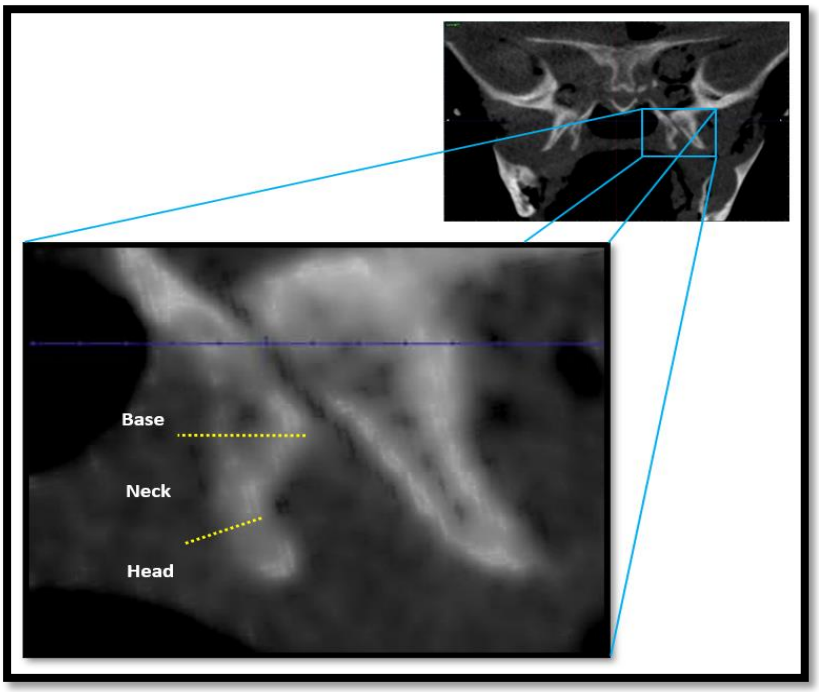

Figure 2.1.1: Linear dimensions of the left pterygoid hamulus according to Putz and Kroyer.[13]

The hook-like structure of the adult pterygoid hamulus, and the factors contributing to this structure was first described in full by Putz and Kroyer.[13] The muscles attaching to the pterygoid hamulus cause an exertive pull on the structure in a dorso-cranial/medial direction. These muscles are the tensor veli palatini, the pterygopharyngeal part of the superior constrictor, the pterygomandibular raphe, the buccinator and according to Putz and Kroyer,[13] the medial pterygoid muscle, even though there is no insertion or origin of this muscle on the pterygoid hamulus according to current literature.

A histological section of the pterygoid hamulus, illustrating a greater thickness of the cortex of the medial lamella than the lateral lamella. In addition to this, they described a latero-caudal tensile pull in the pterygomandibular raphe, which is attached to the pterygoid hamulus at its endpoint. This was not supported in the morphological appearance.[13]

2.1.2 Hard palate

The hard palate is a bony structure that separates the oral and nasal cavities. It is formed by two bones; the palatine processes of the maxillae and the horizontal plates of the palatine bones. It is continuous posteriorly with the soft palate. The hard palate is covered orally with mucosa that is closely bound to the periosteum of the hard palate.[6] The hard palate, also referred to as the secondary palate, forms in utero from the fusion of the intermaxillary segment and the left and right palatine shelves, which are outgrowths of the maxillary prominences.[17]

2.1.3 Surrounding musculature

The **the tensor veli palatini muscle** arises from the scaphoid fossa of the pterygoid process and the spine of the sphenoid bone posteriorly. It is attached to the membranous wall of the Eustachian tube anterolaterally. Fibres of the tensor veli palatini can become continuous with fibres from tensor tympani. The muscle fibres from the origin form a tendon that turns medially around the pterygoid hamulus, gliding over the bursa between the tendon and the pterygoid hamulus. The tendon continues through to the attachment of part of the buccinator muscle to the palatine aponeurosis, to attach to the surface behind the palatine crest on the horizontal plate of the palatine bone. The insertion forms the palatine aponeurosis.[6]

Some of the fibres of tensor veli palatini muscle take origin from the pterygoid hamulus and attach to the lateral cartilage of the Eustachian tube, a condensation of connective tissue lateral to the tubal wall and to a part of Ostmann's fat pad, thereby forming the **dilator tubae**.[6]

The **pterygopharyngeal part of the superior constrictor** (pars pterygo-pharyngea), takes its origin from the pterygoid hamulus, the pterygomandibular raphe, the posterior aspect of the mylohyoid line and the tongue. It inserts onto the pharyngeal tubercle of the occipital bone and the median raphe of the pharynx.[6]

The **pterygomandibular raphe** (the confluence of tendinous fibres of the superior constrictor and the buccinator muscle), takes the form of a thin band that stretches from the posterior end of the mylohyoid line to the pterygoid hamulus.[6]

The **buccinator muscle** occupies the interval between the mandible and maxilla, forming the quadrilateral muscle of the cheek. Its posterior border is attached to the anterior margin of the pterygomandibular raphe. It is deeply placed posteriorly in the plane of the medial pterygoid plate, medial to the mandibular ramus. The anterior border curves out from behind the first molar tooth to lie in the submucosa of the cheeks and lips. The superior border is attached to the alveolar processes of the maxilla. The inferior border is attached to the alveolar processes of the mandible. The attachments of both the superior and the inferior borders are opposite of the molar teeth.[6]

Furthermore, some of the fibres of the buccinator muscle originate from a fine tendinous band that stretches over the interval created between the mandible and the pterygoid hamulus; finding their attachments at the tuberosity of the maxilla on one side, and the upper end of the pterygomandibular raphe on the other side. The tendon of tensor veli palatini muscle pierces the buccinator muscle on its way to its attachment at the soft palate, at the pharyngeal wall where there is a small space behind the tendinous band.[6]

The fibres of the buccinator muscle converge towards the modiolus at the angle of the mouth. At the modiolus, some of the fibres from the buccinator muscle form a

decussation. The pterygomandibular (central) fibres intersect at the modiolus, where the lower fibres cross to the upper part of orbicularis oris and the upper fibres cross to the lower part. In contrast, the maxillary (highest) and mandibular (lowest) fibres continue to enter the corresponding lips without this crossover. A substantial amount of the buccinator muscle fibres attach internally to the submucosa.[6,18]

2.2 Pathology

The pterygoid hamulus is an important landmark when considering the muscles that find their attachment on this structure. The tendon of the tensor veli palatini muscle is one of those that wind around the pterygoid hamulus, situated in a groove on the surface thereof. A synovial bursa is formed between the tendon and the bony structure.[12]

Hamular bursitis is an inflammation of the synovial bursa between the tendon of the tensor veli palatini muscle and the pterygoid hamulus.[19] The exact aetiology of this pain disorder is not known, but swallowing a large bolus or having a more prominent pterygoid hamulus may make it more prone to mechanical trauma. Pain is therefore a prominent symptom of hamular bursitis.[12]

Hamular bursitis is diagnosed by way of careful examination of the area. Physical presentation is an erythematous appearance of the area directly over the pterygoid hamulus. This area will also have tenderness on palpation, which disappears after anaesthetic infiltration of the area. Furthermore, radiographs of the pterygoid hamulus can determine if the pterygoid hamulus is fractured or if there is an osteophyte present.[12]

Treatment can be conservative or surgical. Conservative treatment involves the removal of the cause of the trauma, if still present. Synthetic cortisone is injected into the region of the pterygoid hamulus and anti-inflammatory medication is prescribed to the patient until re-evaluation can be done after two weeks. When conservative treatment is unsuccessful, surgery is considered to either remove osteophytes or remove excess fibrous enlargement and slit the bursa to allow for free movement of the tendon.[12]

An **elongated pterygoid hamulus** presents largely with the symptom of pain. It can be diagnosed by way of visually checking for a firm swelling or enlargement under the mucosa of the soft palate.[12] It can remain undiagnosed for many years, being misdiagnosed as phantom or psychological pain.[9,20-21] Treatment consists of surgical resection after blunt dissection is used to find the pterygoid hamulus (Figures 2.2.1 to 2.2.3).

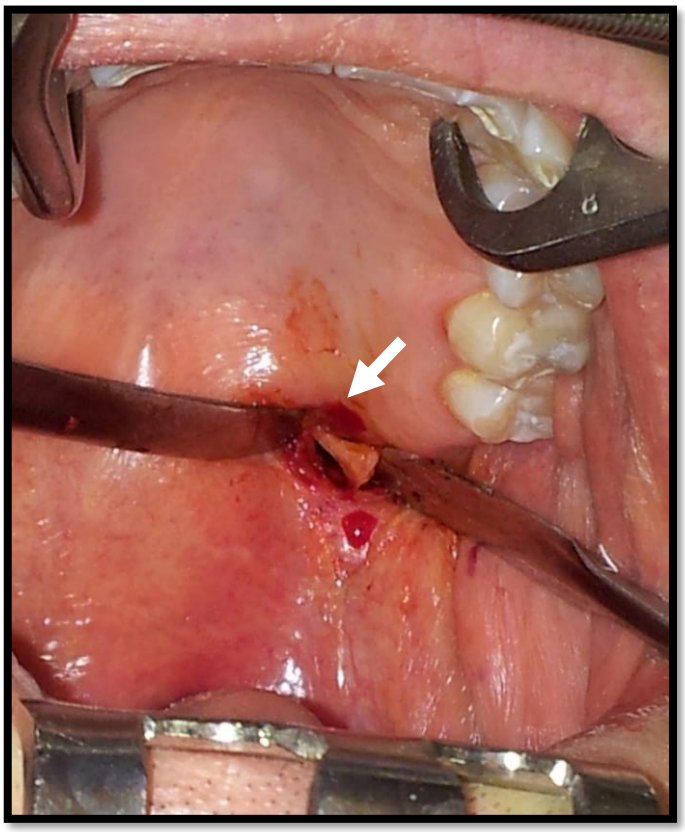

Figure 2.2.1: An elongated hamulus in situ after exposure.[4]

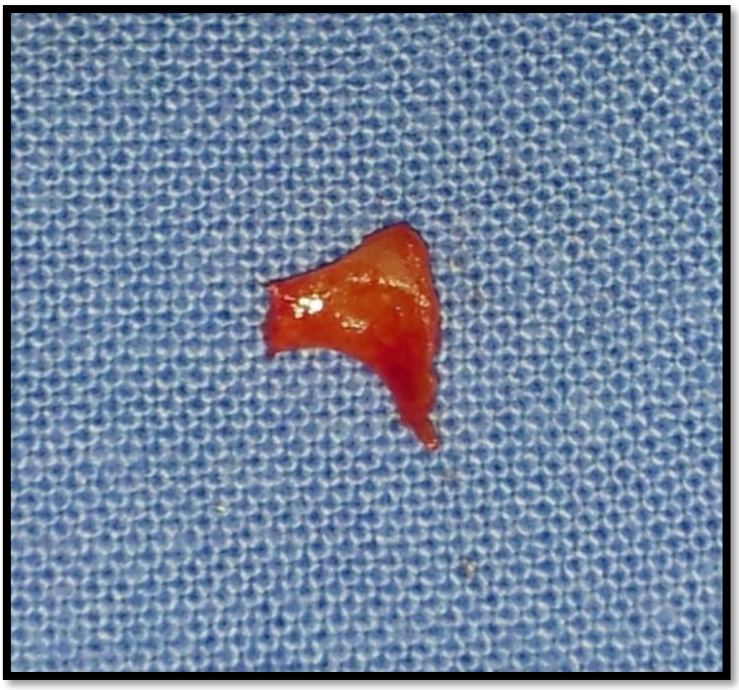

Figure 2.2.2: The removed tip of the elongated pterygoid hamulus.[4]

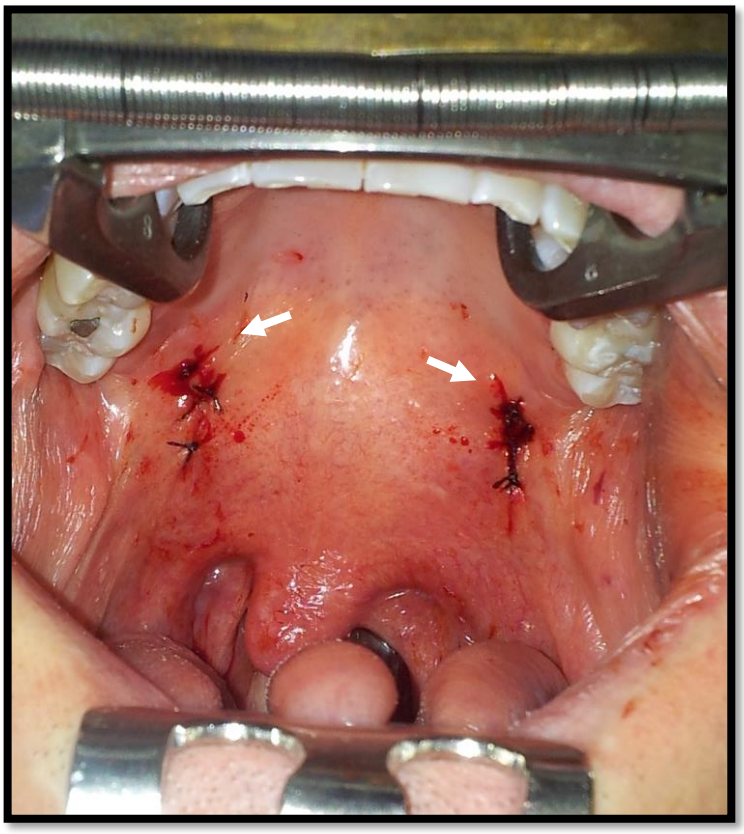

Figure 2.2.3: Sutures indicating where the elongated hamuli were removed.[4]

A **cleft palate** occurs when there is an opening in the palate of the mouth that extends into the nasal cavity. A cleft lip is an opening that extends from the upper lip into the nose. A cleft palate and/or lip occurs when the tissue of the face doesn't fuse during foetal development. In cleft palate patients, it is found that they suffer more from otitis media, as the functionality of the muscles that hook around the pterygoid hamulus is decreased and it does not open the Eustachian tube effectively.

Cleft lip and/or palate is repaired by way of surgery, the surgical technique depends on the severity of the cleft and the surgeons personal preference.[22] One of the techniques include placing a tensor stitch through the periosteum on the medial side of the pterygoid hamuli as part of the surgical closure of the cleft. This is in order to keep them in position during development, increasing the normal function on the Eustachian tube.

2.3 Similar studies

Data available on the anatomy of the pterygoid hamulus is not commonly found. For this study, the only articles found on this subject were used as reference; Putz and Kroyer,[13] Krmpotić-Nemanić *et al.*,[14] Orhan *et al.*[15] and Rajion *et al*.[16] Although some errors were found in Putz and Kroyer's article, Krmpotić-Nemanić *et al.*[14] and Orhan *et al.*[11] used different information in their articles to show these errors. A comparison of the results found in each study regarding the relevant measurements is outlined in table 6.6.1.

Putz and Kroyer[13] reported on the functional anatomy of the pterygoid hamulus in a German population by examining skulls and their muscle attachments. The subsequent two articles listed after Putz and Kroyer[13] used this article as a reference when conducting their research. These articles differed in some of the information reported by Putz and Kroyer[13].

The results that Putz and Kroyer[13] obtained when measuring the pterygoid hamulus were as follows; the average length was 7.2mm in the sagittal plane, the average transverse diameter was 2.3mm, the average sagittal diameter was 1.4mm, the

transverse distance between the two hamuli was 26 to 36.9mm, the inclination in the frontal plane was 58° and the inclination in the sagittal plane was 75°.

The authors reported that tensor veli palatini does not only use the hamulus to change direction but also attaches to it, which in the contemporary literature, at that time, had not been reported. It has since been correctly reported in more modern and updated literature, such as anatomy textbooks available today[6]. The erroneous information reported by this article, was that the pterygoid hamulus would stay constant throughout development, only growing larger until adulthood is reached, after which it remains constant.

Jelena Krmpotić-Nemanić, Ivan Vinter and Ana Marušić[14] reported on the relations of the pterygoid hamulus and the hard palate on a Croatian population using articulated and disarticulated skulls. Their research reported that the pterygoid hamulus and the surrounding structures change with age, in contrast to Putz and Kroyer.[13] They further reported that these changes occur in concurrence with changes in function of the pharyngeal and palatal muscles during deglutition. Their study focused on the clinical implications of sleep apnoea and snoring.

The study of Krmpotić-Nemanić *et al*.[14] reported more specifically on the clinical application on the soft palate. They did measure different structures, such as the width of the hard palate in the choanal region. They also measured the length of the hamulus, the inclination of the hamulus in the plane perpendicular to the lateral limit of the choana and the distance between the tips of the hamuli. These measurements, unlike Putz and Kroyer,[13] were done on children, adults and the elderly.

They found the length of the hamulus to be 3.6±1.5mm in children, 6.9±1.7mm in adults and 5.0±1.9mm in the elderly. The adult length is similar to that reported by Putz and Kroyer.[13] The inclination of the hamulus from the plane perpendicular to the lateral limit of the choana was found to be 19.6±12.1° in children, 35.9±13.7° in adults and 19.7±1.9° in the elderly. Lastly, the distance between the tips of the hamuli was found to be 31.0±3.7mm in children, 38.0±2.7mm in adults and 32.7±3.9mm in the elderly.

They continued to report on the change in shape of the hamulus throughout the three recorded stages of development. They found that in children, the shape was short, massive and hook-like. In adults the shape was long and slender with a furrow on the base and a strong tip, along with a lateral inclination. In the elderly the shape was found to be shorter and less laterally inclined. They also noted that the mechanical load of the buccopharyngeal raphe is possibly responsible for the elongation of the hamulus in adults.

Kaan Orhan, Bayram Sakul, Ulas Oz and Burak Bilecenoglu[15] conducted a study to evaluate the pterygoid hamulus morphology using Cone Beam Computed Tomography (CBCT) in a Turkish population. They reported on all the possible abnormalities that can occur because of an oddly shaped pterygoid hamulus. They further confirmed the results of Krmpotić-Nemanić *et al.*[15]

They used the case study of a 26-year old female with soft palate pain of duration of 9 months after a traumatic removal of the right maxillary third molar. This led them to conduct a study of the pterygoid hamulus in their population. They used the craniofacial CBCT scans of 198 subjects in a retrograde investigation. No preference in regard to sex was made when considering the sample choice.

They measured the length in a similar fashion to Putz and Kroyer,[13] from the junction of the medial pterygoid plate with the pterygoid hamulus through to the hamulus tip. The width of the pterygoid hamulus they measured as the distance between the most prominent points on the hamulus in a coronal plane. Additionally, they measured the inclination of the pterygoid hamulus in both the coronal and sagittal planes according to the horizontal plane that Putz and Kroyer[13] stated. They classified the inclination in the coronal plane as lateral or medial and the inclination in the sagittal plane as anterior and posterior.

Their results indicated that the length of the pterygoid hamulus was 5.48±1.94mm on the left sides and 5.40±2.0mm on the right sides. The width of both the left and right sides were found to measure 1.72±0.94mm and 1.87±1.17mm respectively. No significant differences were observed between the left and right sides with these measurements. They found all the hamuli to be inclined towards the lateral side in the

coronal plane. In the sagittal plane they observed that 21.7% of the hamuli were inclined anteriorly and 78.3% were inclined posteriorly on the left side. On the right side however, the inclination toward the anterior was 22.7% and the inclination towards the posterior was 77.3%. The angle between the posterior nasal spine and the tip of the hamulus was found to be 33.4±2.34° for the left and 34.3±2.18° for the right.

The results showed no significant difference between male and female in localization and measurements of the pterygoid hamuli. They divided the sample group into two subgroups according to age, creating a 22-to-55 year old group and a 55 year and older group. They found that the 55 year and older group measured shorter hamuli. Confirming the results found by Krmpotić-Nemanić *et al.*,[14] they observed that the position and morphology of the pterygoid hamulus is closely related to the function of the tensor veli palatini, which affects the width of the hard palate during swallowing. In addition, they found that the inclination of the pterygoid hamulus is responsible for better tension of the palatal aponeurosis.

Zainul Rajion, Ali Al-Khatib, David Netherway, Grant Townsend, Peter Anderson, Neil McLean and Ab Rani Samsudin[16] conducted a study to assess the skeletal components of the nasopharyngeal area in patients with either cleft lip and/or palate and non-cleft patients, as well as quantifying anatomical variations. This was achieved by way of CBCT scans.

Rajion *et al.*[16] conducted their study based on the fact that little attention has been given to the importance of the morphology of the nasopharynx when evaluating the function of the velopharyngeal components. This is because of the limitations of the methods that are available to take measurements.

Unlike the previous two articles mentioned, this article did not build on Putz and Kroyer's results. More specific measurements relating to their research objectives were made, as they looked at both non-cleft infants and infants with various classifications of cleft lip. Although the Raijon *et al.*[16] study most closely resembles the direction that this study took, there was only one common measurement between their study and ours. Rajion *et al.*[16] conducted their study on a Malaysian population

of 29 patients within the age range of 0 to 12 months, 17 of these patients had various forms of cleft lip and palate and 12 were non-cleft patients.

Furthermore, they compared males and females, with data indicating that select measurements, which were not used in this study, were larger in males than in females. The inter-hamular process distance is defined as the distance measured from the tips of the left and right hamular processes of the medial pterygoid plates of the sphenoid. They found the inter-hamular distance to be 22.3±0.59mm for the non-cleft patients.

Their results showed that there is an increased nasopharyngeal space in patients with cleft lip and palate that may lead to compression of the nasopharyngeal structures. Alterations of the medial pterygoid plate and the pterygoid hamulus may lead to changes in the orientation and origin of the tensor veli palatini muscle which in turn leads to changes in its function.

2.4 Corrective procedure: Tensor sling procedure

The tensor sling procedure is a cleft palate corrective procedure developed and utilized by Prof. Bütow[23]. This procedure aims to allow for forward growth of the developing jaw, while the two pterygoid hamuli are forced more medial using a tensor stitch. Post-operative observations in cases where the tensor sling procedure was performed suggested that Eustachian tube functionality was better than in most other corrective surgeries. Incidences of otitis media was also significantly lower. The improved Eustachian tube function is due to the tensor stitch pulling the pterygoid hamuli medially, thereby relieving lateral pressure on the Eustachian tube.[23]

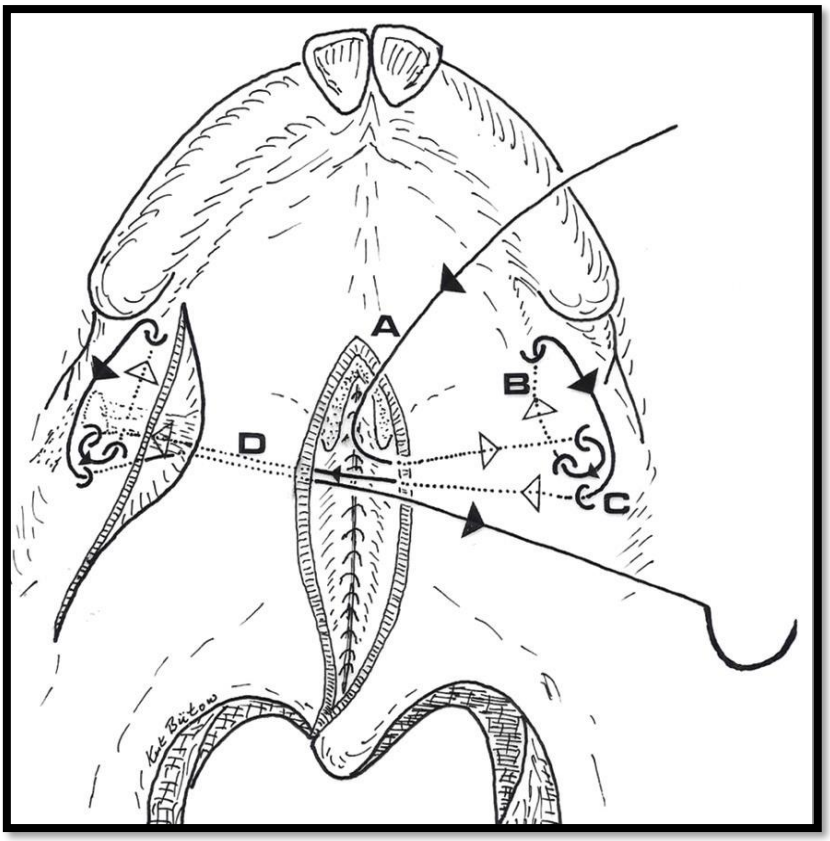

Figure 2.4.1: A visual representation of the tensor sling procedure showing the path that is taken by the stiches. Solid lines indicate where the stitches are above the surface, and dotted lines indicate where the stitches are beneath the mucosa and periosteum. (A) Insertion site of the tensor stitch. (B) Site of the maxillary tuberosity. (C) Pterygoid hamulus of the medial pterygoid plate. (D) Crossover of the stitch to the opposite side.[23]

In this procedure (Figure 2.4.1), the deep cleft has already been corrected, with the overlaying mucosa still open. The two sides of the mucosa that forms the cleft is then cut along their medial border to separate the nasal part of the mucosa from the oral part. The two nasal parts are then joined to separate the nasal cavity from the oral cavity. Thereafter, the right and left muscles of the palate are loosened and attached to each other.

The stitch is inserted through the opening in the mucosa, pulled through laterally beneath the soft tissue (mucosa) and pulled to the surface, looping around the medial pterygoid plate on the surface of the mucosa. It is then reinserted underneath the mucosa and deep to the periosteum, medial to the medial pterygoid plate and pulled

anteriorly until the maxillary tuberosity is reached where the stitch is then pulled to the surface again, coursing posteriorly. The stitch is then reinserted through the mucosa and periosteum posterior to the medial pterygoid plate.

Thereafter, the stitch is progressed to the opposite side of the mouth, following a similar course as on the opposite side. After reaching the opposite side, the stitch is brought through to the surface, hooked around the medial pterygoid plate, and reinserted through the mucosa and deep to the periosteum medial to the medial pterygoid plate. It is progressed anteriorly and re-emerges at the surface medial to the maxillary tuberosity, looped around the tuberosity laterally, then travels over the surface posteriorly. It is then reinserted through the mucosa and periosteum posterior to the medial pterygoid plate and pulled through the gap in the mucosa.

The ends of the stitches are then pulled together and tied, forcing the medial pterygoid plates towards each other in the median. Lastly the oral parts of the mucosa (left and right) of the cleft are sutured together, closing it.[23]

3. Aim

The aim of this study was to provide a comprehensive anatomical description of the neonatal pterygoid hamulus in a South African population. This will ensure baseline parameters against which the effect of reparative cleft palate surgery and other pathologies of the Eustachian tube, surrounding musculature and pterygoid hamulus can be measured.

3.1 Research objectives

In order to determine the effect of the morphometry of the pterygoid hamulus on the surrounding structures during surgery, the pterygoid hamulus' parameters need to be defined in a quantitative manner.

Therefore, the following research objectives were set:

1. To measure the length of the pterygoid hamulus (LH)
2. To measure the width of the pterygoid hamulus in the coronal plane (WHC)
3. To measure the width of the pterygoid hamulus in the sagittal plane (WHS)
4. To measure the distance to the posterior nasal spine (PNS)
5. To measure the inclination of the pterygoid hamulus in the coronal plane (IC)
6. To measure the inclination of the pterygoid hamulus in the sagittal plane (IS)
7. To measure the inter-hamular distance (IHD)

4. Materials and methods

4.1 Setting

All scans and measurements were conducted in the Oral-and-Dental Hospital at the University of Pretoria, South Africa.

4.2 Study design

This study consists of a cross sectional, descriptive design. Quantitative data were measured and collected from cadaveric specimens and statistically analysed.

4.3 Sample size

The sample for this study consisted of 74 formalin-fixed neonatal cadavers, of which 45 were male and 29 were female. These cadavers were housed in the Department of Anatomy of the University of Pretoria. Of these 74 neonatal cadavers 18 were white and 56 were black. Only cadavers between the age of zero and 28 days, with no observable abnormalities concerning the head and neck, were scanned using a CBCT scanner. Scans that showed damage to the pterygoid hamulus were not used. Table 4.3.1 outlines the demographic data of the sample. Only South African cadavers were included.

Table 4.3.1: Demographic details of the sample

	N	Mean	SD	Min	Max	Range
Age (days)	73	2.3	5.7	0.00	28	28
Height (m)	72	0.40	0.071	0.29	0.56	0.27
Weight (kg)	74	1.5	0.78	0.60	4	3.4

4.4 Procedure for CBCT scanning

After approval from the Head of the Department of Anatomy was obtained, the neonatal cadavers were transported from the anatomical storage facilities to the Oral-and-Dental Hospital at the University of Pretoria, Prinshof campus, using a sealed and covered container.

The neonates were placed in a standardised position and were stabilized with an industrial lab stand with clamps, in combination with the head positioning equipment of the scanning machine (Figure 4.4.1). The neonates were clamped at the level of the axilla or waist, positioning the cadaver as vertically as possible. The head was positioned so that the chin of the neonate was secured in the chin rest of the head positioning equipment of the scanning machine. Dr. A Uys from the Department of Radiology in the Oral-and-Dental Hospital scanned the heads at 90kV, 8.0mA with the Planmeca's ProMax3D Max machine to capture the 2D sectional scans of the pterygoid hamulus.

Figure 4.4.1 Standardised position that the neonate is set up within the CBCT machine.

4.5 Quantitative data measurements

The method of measurement as defined by Orhan *et al.*[15] based on Putz and Kroyer[13] and Krmpotić-Nemanić *et al.*[14] was used for this study whenever the previously mentioned authors specified the procedure of measurement in a way that could be completely duplicated.

A cursor-driven pointer was used to identify landmarks on the CBCT scans as displayed on the Planmeca Romexis 4.6.0.R program. Romexis gave a full screen view of the enlarged areas for easier determination of the identified points. This program measures distances between two selected points on the screen in millimetres. The length of the pterygoid hamulus (LH), the width of pterygoid hamulus in the coronal plane (WHC) and the inter-hamular distance (IHD) were taken in the coronal plane. An example of a scan of the sphenoid bone in the coronal plane is given in the figure below (Figure 4.5.1).

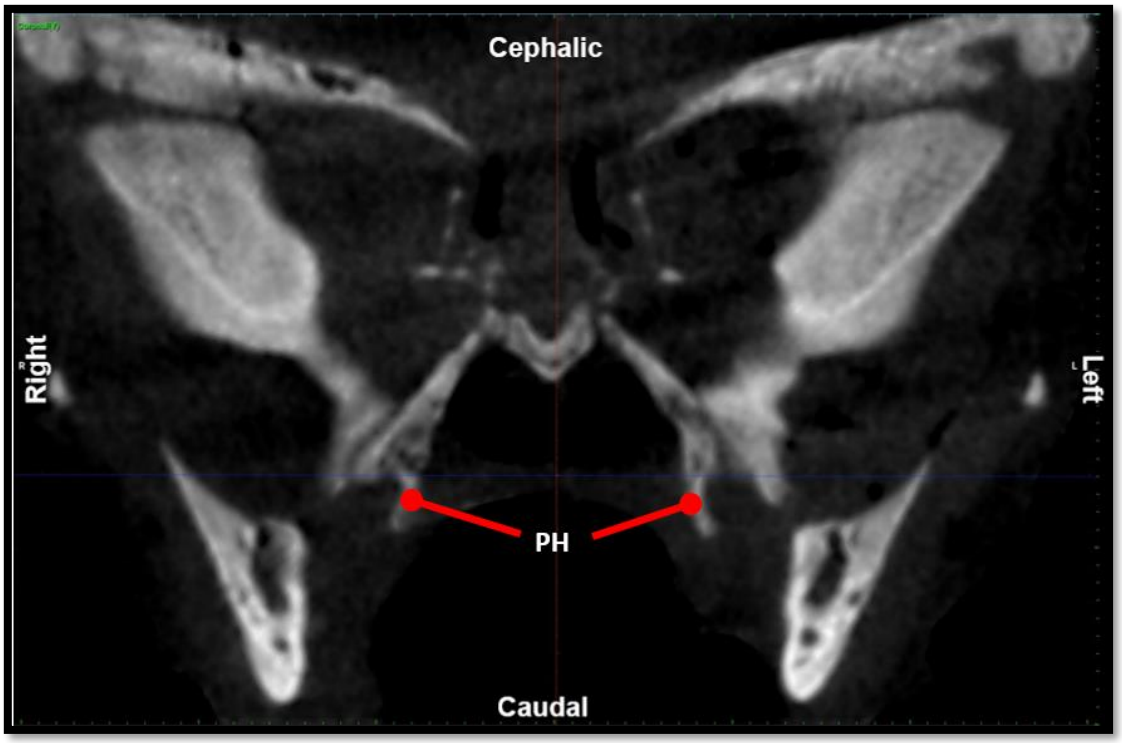

Figure 4.5.1: CBCT scan of a neonatal cadaver, showing most of the sphenoid bone in the coronal plane on the section where the pterygoid hamulus (PH) was best observed.

In order to standardise each measurement technique for all measurements that were taken in the three sections (coronal, sagittal and axial), the horizontal (axial) plane was established in the sagittal plane (Figure 4.5.2), with the functions available on the Romexis program. This horizontal plane was established by angling the CBCT scan until the anterior and posterior nasal spines were aligned on the line demarcating the axial plane. This would ensure that the axial plane on the coronal plane would be aligned with the anterior -and posterior nasal spines.

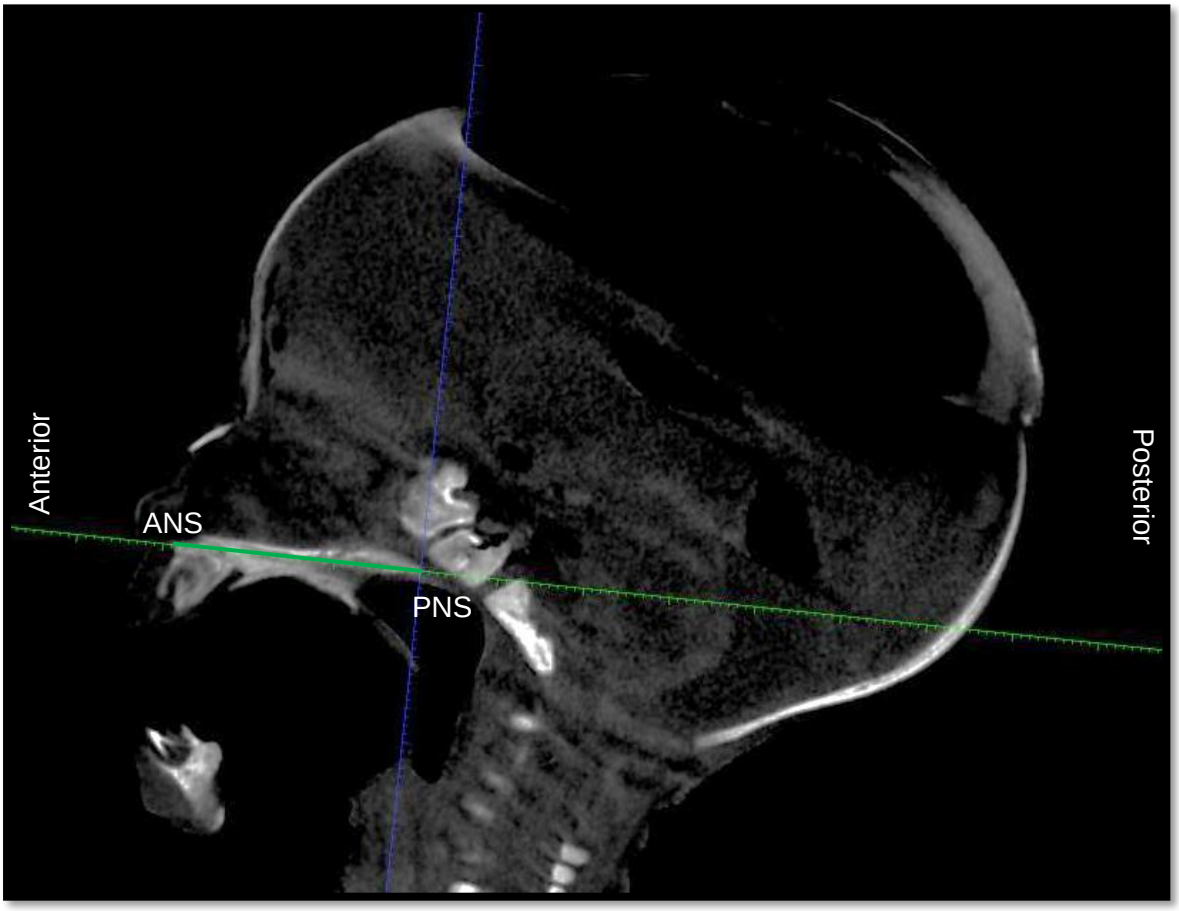

Figure 4.5.2: Horizontal (axial) plane in the sagittal section running through the anterior nasal spine (ANS) and the posterior nasal spine (PNS). The green line indicates the axial plane.

The length of the pterygoid hamulus measurement (AB) was taken from the junction between the base and the neck of the hamulus (point A), to the most inferior point of the tip of the hamulus (point B). To standardize this measurement, a line was drawn between the most lateral and medial point of the base-neck-junction (CD).

The midpoint of this line (A) was established by which to measure the LH, on both sides (Figure 4.5.3).

The width of the pterygoid hamulus in the coronal plane was measured as the distance between the two most prominent points on the base or neck of the hamulus (CD, in this case), on both sides. The inter-hamular distance (BE) was measured as the distance between the most inferior tips of the right and left pterygoid hamulus (Figure 4.5.3).

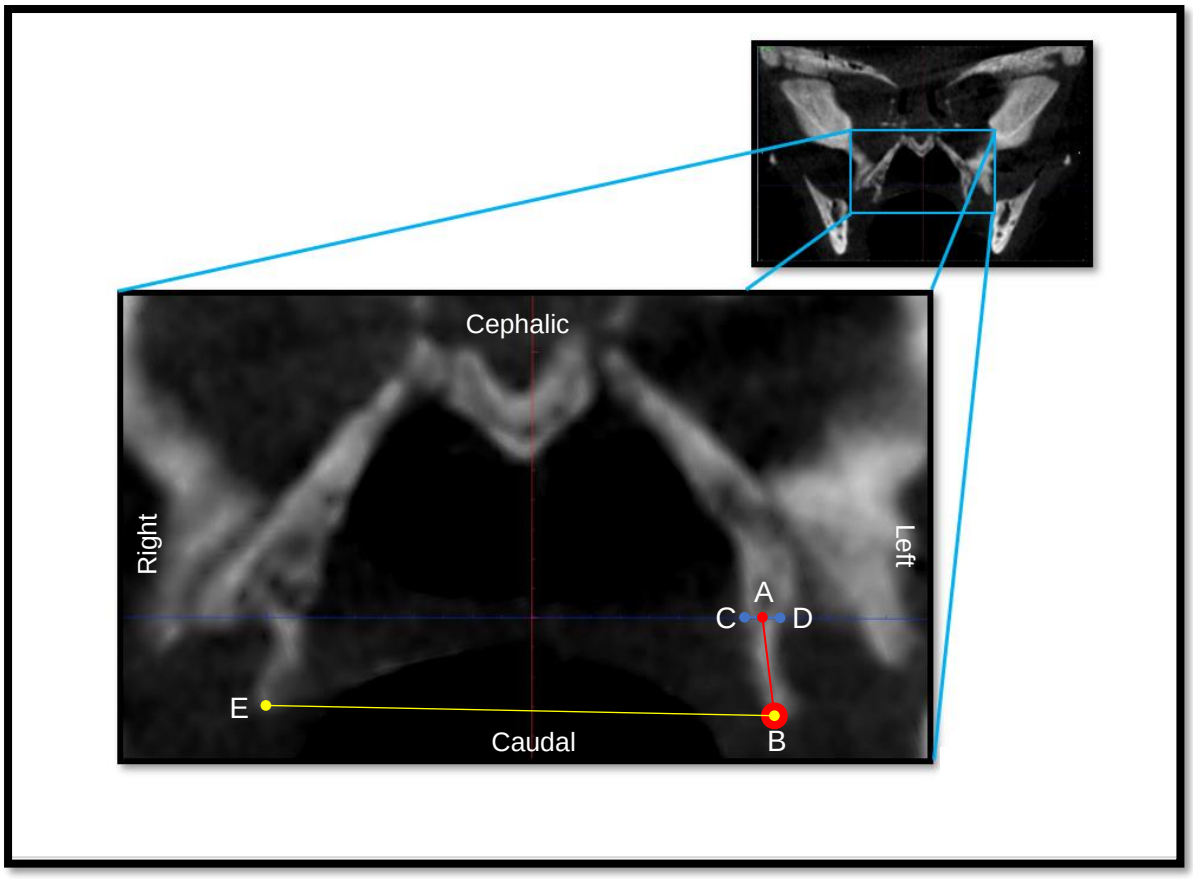

Figure 4.5.3: Enlarged CBCT scan in the coronal plane indicating the pterygoid hamuli. (A) Midpoint of base-neck junction of hamulus. (B) and (D) Most inferior point on the tip of the hamulus. (C) Most medial point on the base-neck junction of the left hamulus. (D) Most lateral point on the base-neck junction of the left hamulus.

The width of the pterygoid hamulus in the sagittal plane (FG) was determined by measuring the distance between the most anterior point on the hamulus (F), and the most posterior point on the hamulus (G) at its widest parts, usually at the base or the head (Figure 4.5.4).

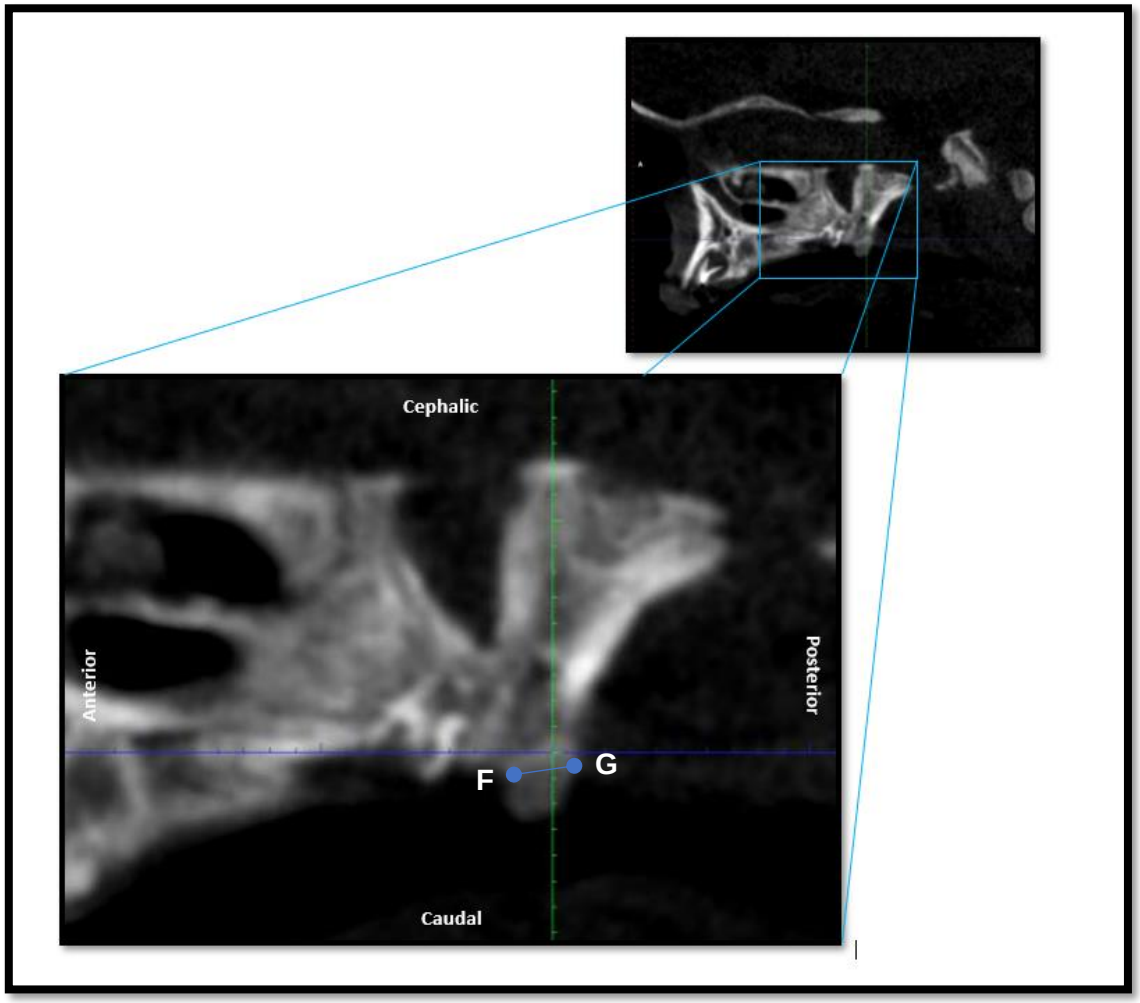

Figure 4.5.4: Enlarged CBCT scan in the sagittal plane indicating the left pterygoid hamulus. (F) Is the most anterior point, and (G) is the most posterior point.

The distance from the pterygoid hamulus to the posterior nasal spine, on both sides, was measured from the most inferior tip of the pterygoid hamulus (H) to the tip of the posterior nasal spine (I). This measurement was made on an oblique horizontal plane, levelled by angling the horizontal plane until both points were observed (Figure 4.5.5).

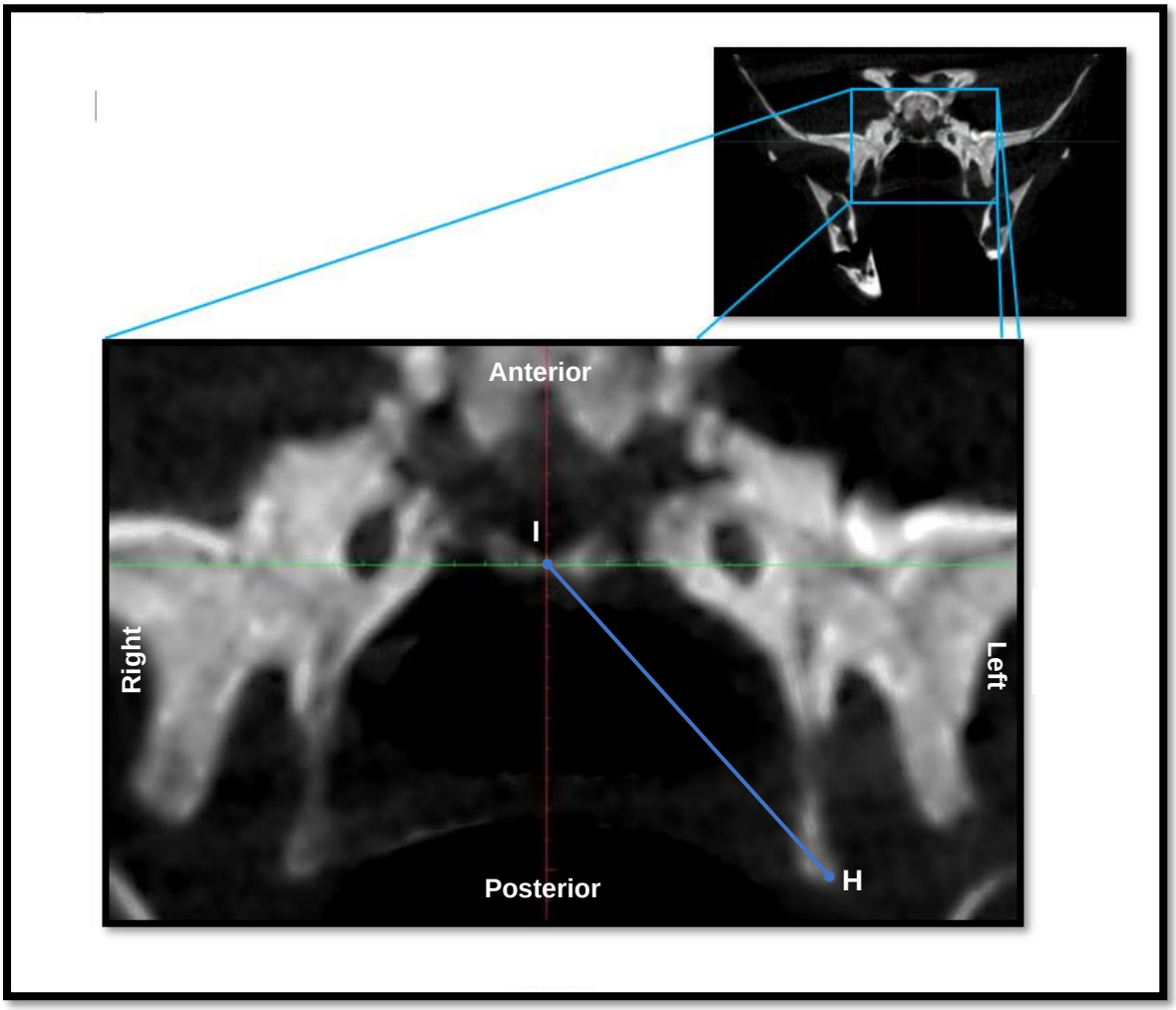

Figure 4.5.5: Enlarged CBCT scan in the axial plane indicating the pterygoid hamuli and the posterior nasal spine. (H) The most inferior point on the tip of the hamulus. (I) The posterior nasal spine.

For the measurement of the inclination in the coronal plane (IC), a horizontal line (JK) was established by connecting the right (J) and left (K) base-neck-junctions of the pterygoid hamuli. Another line (KL) was established from the midpoint of the base-neck junction of the pterygoid hamulus (K), to the most inferior point on the tip of the hamulus (L). The angle between these two lines was then measured in degrees (°). This means that the medial angle for both right and left sides were measured (Figure 4.5.6).

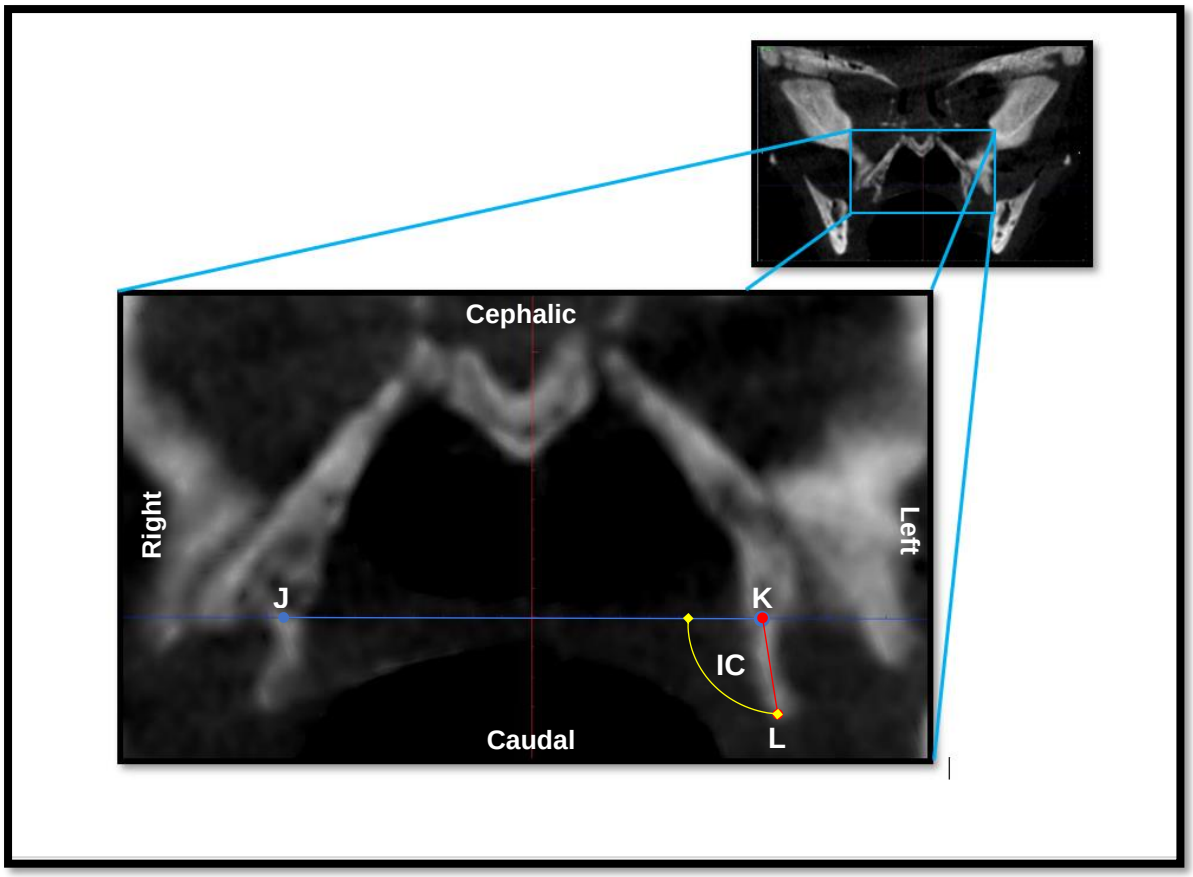

Figure 4.5.6: Enlarged CBCT scan in the coronal plane indicating the pterygoid hamuli. (J) Midpoint of base-neck junction of hamulus on the right hamulus, and (K), the midpoint on the left. (L) The most inferior point on the tip of the left hamulus. (IC) The medial angle between the line connecting the right and left base-neck junctions, and the length of the hamulus.

For the measurement of the inclination of the pterygoid in the sagittal plane, a standardised horizontal plane is especially important. The horizontal plane has already been established in figure 4.5.2. The dark blue line shown in figure 4.5.7, is the horizontal plane. In order to establish the second axis by which the inclination is measured, certain landmarks need to be established. To establish the length of the pterygoid hamulus (OP), the midpoint of the base of the hamulus (O) is established by first finding the most anterior (M) and posterior (N) points on the base of the hamulus. The midpoint between these two is then used.

The length of the hamulus was measured from the midpoint of the base (O), to the most inferior point on the tip of the hamulus (P). The inclination of the pterygoid

hamulus in the sagittal plane (IS) is then measured as the angle between the length of the hamulus (OP) and the horizontal plane (Figure 4.5.7).

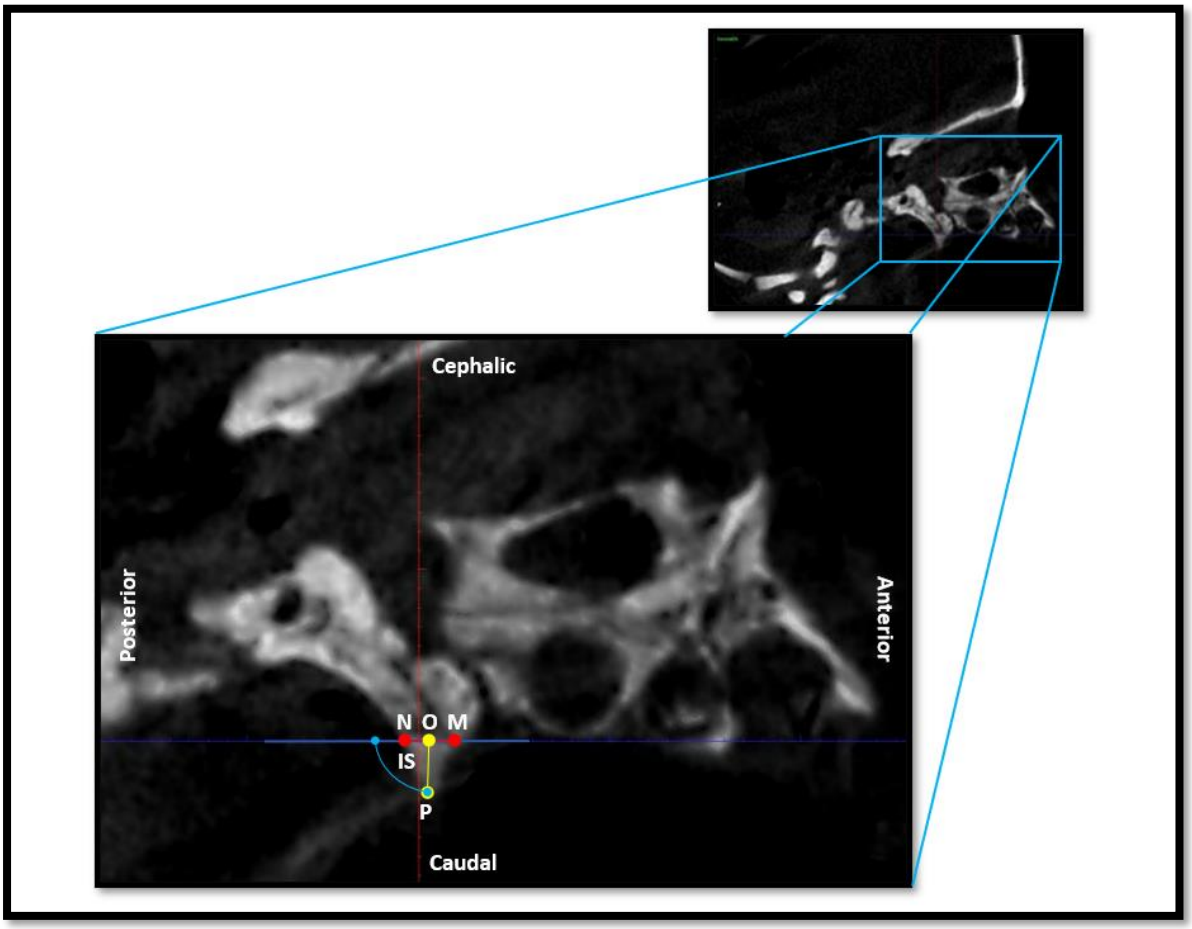

Figure 4.5.7: Enlarged CBCT scan in the sagittal plane indicating the pterygoid hamulus. (M) The most anterior point on the base of the hamulus. (N) The most posterior point on the base of the hamulus. (O) The midpoint of the base of the hamulus. (P) The most inferior point on the tip of the hamulus. Dark blue line indicates the horizontal plane. (IS) The angle between the horizontal plane.

4.6 Statistical analysis

The measurements were captured in Microsoft Excel 2019 spreadsheets (see Appendix A.1). Statistical testing of the data was performed using IBM SPSS version 21. Descriptive statistics were used to describe the data obtained from the sample, this includes the mean, median (median was only to be used if there was a “skew distribution” of the collected data points), standard deviation, minimum and maximum of all the measurements. A range with a confidence interval of 95% was also

calculated. In order to establish if the data was normally distributed or skew, a Shapiro-Wilk test was done. Next, standardised scores (Z-Scores) were used to establish which data skewed the distribution. The Z-scores of the skewed data were used to remove any outliers with a value of more than 2.5 or less than -2.5.

Comparisons between groups/measurements (i.e. left *vs*. right, black *vs*. white) were made using a paired t-test (when the values were normally distributed) or a Wilcoxon signed raked test (when the values were skewed). The relationship (strength of correlation) between the collected measurements and the demographic details (i.e. weight and height) was calculated using Pearson's or Spearman's rho (r) depending on the data distribution.

The dependent variables were the measurements taken, while the independent variables were the weight and body length of the sample. Correlation coefficient (r-values) between 0.7 and 1.0 is considered a high (strong) correlation between the independent variables and the measured distance(s), a moderate correlation has an r-value between 0.5 and 0.7, while any r-value less than 0.5 is considered as a poor correlation. For any correlation coefficient that exceeds or is equal to 0.7, a linear regression analysis was carried out.

The aim of intra- and inter-observer error tests is to test the accuracy and repeatability of the measurements. The intra-observer error determination was repeated at a later date by the primary investigator and determines whether the observer can repeat his/her own results (measures the accuracy of the results). The supervisor repeated the measurements, without any influence from the primary investigator. This determines the inter-observer error and tests whether the results can be reproduced (measures the repeatability of the results).

This will require both the primary investigator and supervisor to repeat the measurements that were taken for the CBCT scans, where both the left and the right sides of 26 (25 in the case of the supervisor) randomly selected scans were measured again. The set of measurements were interpreted using the Bland and Altman method. This process of comparison allows for future addition to the data set or comparisons with other data sets.

4.7. Ethical considerations

The study has obtained approval from the MSc committee and the research ethics committee of the Faculty of Health Sciences, University of Pretoria (ethics reference No: 667/2019). The ethics approval letter can be found in appendix F.

Although certain parameters of the cadavers were known, no information identifying individuals were made known and therefore remained confidential. The data was tabulated, but kept confidential and used for statistical purposes only.

Only cadaveric material stored in the Department of Anatomy, School of Medicine, Faculty of Health Science, University of Pretoria, was used in this study. All the cadavers were obtained legally and scanned under the rules and regulations stated within the South African National Health Act 61 of 2003.

5. Results

5.1 Test for normality

In order to establish the database, the data collected had to be adapted in order to be comparable and to establish differences wherever found. In order to create a larger sample of data, left and right measurements had to be compared in order to establish if they could be combined.

To do this, descriptive statistical analysis (Appendix A.2) was performed from the data collection sheet (Appendix A.1). A Shapiro-Wilk test (Appendix A.3) was then performed and revealed that measurements width of the right pterygoid hamulus in the coronal plane (WHCR), inclination of the right pterygoid hamulus in the sagittal plane (ISR), width of the left pterygoid hamulus in the coronal plane (WHCL) and the distance from the tip of the left pterygoid hamulus to the posterior nasal spine (PNSL) had p-values less than 0.05, indicating that the null hypothesis of equal distribution was rejected. Other factors, such as the skewness and kurtosis of the data, were also evaluated. Measurements that had a skewness greater than 1.0 and kurtosis greater than 2.0 were not considered normally distributed.

Next, the measurements had to be standardised so that a more normally distributed data set could be established. This was done by evaluating the Z-scores of the individual measurements, and then removing values that were greater than 2.5 or less than -2.5 from the data set. After the removal of these Z-scores the distribution of the measurements was recalculated (Table 5.1.1).

Table 5.1.1: Standardised descriptive statistical analysis after the removal of measurements corresponding to outlying Z-scores

	N	Mean		Std. Deviation	Min.	Max.	Range
		Statistic	Std. Error				
LHR	73	2.56	0.0543	0.464	1.71	3.76	2.05
WHCR	72	1.03	0.0248	0.210	0.800	1.60	0.800
WHSR	74	1.79	0.458	0.394	0.82	2.63	1.81
PNSR	74	11.2	0.198	1.70	7.96	15.2	7.28
ICR	73	107	1.13	9.69	88.3	131	42.9
ISR	74	88.9	2.30	19.8	56.3	137	81.0
LHL	73	2.51	0.0592	0.506	1.60	3.61	2.01
WHCL	73	1.05	0.0268	0.229	0.800	1.61	0.810
WHSL	74	1.81	0.0522	0.449	1.00	2.91	1.91
PNSL	74	11.1	0.207	1.78	7.78	15.2	7.38
ICL	72	108	1.24	10.5	82.3	129	47.0
ISL	74	86.8	2.22	19.1	40.6	131	90.6
IHD	74	16.9	0.356	3.06	11.0	24.2	13.2

Key	Description	Key	Description
LHR	Length of the right pterygoid hamulus	**LHL**	Length of the left pterygoid hamulus
WHCR	Width of the right pterygoid hamulus in the coronal plane	**WHCL**	Width of the left pterygoid hamulus in the coronal plane
WHSR	Width of the right pterygoid hamulus in the sagittal plane	**WHSL**	Width of the left pterygoid hamulus in the sagittal plane
PNSR	Distance from the tip of the right pterygoid hamulus to the posterior nasal spine	**PNSL**	Distance from the tip of the left pterygoid hamulus to the posterior nasal spine
ICR	Inclination of the right pterygoid hamulus in the coronal plane	**ICL**	Inclination of the left pterygoid hamulus in the coronal plane
ISR	Inclination of the right pterygoid hamulus in the sagittal plane	**ISL**	Inclination of the left pterygoid hamulus in the sagittal plane
IHD	Pterygoid inter-hamulus distance		

A second Shapiro-Wilk test, as well as evaluating the skewness and kurtosis (Table 5.1.2), was conducted with the measurements corresponding to the removed Z-scores having been removed. The test revealed that the measurements WHCR, WHCL and PNSL had a p-value of less than 0.05, and therefore were not normally distributed.

Table 5.1.2: Shapiro-Wilk test, Skewness and Kurtosis of standardised measurements, with p-values indicating measurements that could not be compared using a paired t-test highlighted (not normally distributed)

	Shapiro-Wilk			Skewness		Kurtosis	
	Statistic	df	P-value	Statistic	Std. Error	Statistic	Std. Error
LHR	0.977	67	0.235	0.244	0.293	-0.635	0.578
WHCR	0.882	67	0.000	0.559	0.293	-0.629	0.578
WHSR	0.974	67	0.183	0.125	0.293	-0.282	0.578
PNSR	0.975	67	0.193	0.188	0.293	-0.822	0.578
ICR	0.984	67	0.518	0.169	0.293	-0.422	0.578
ISR	0.966	67	0.067	0.409	0.293	-0.479	0.578
LHL	0.980	67	0.338	0.0880	0.293	-0.763	0.578
WHCL	0.874	67	0.000	0.910	0.293	0.0900	0.578
WHSL	0.978	67	0.279	0.247	0.293	-0.314	0.578
PNSL	0.961	67	0.034	0.386	0.293	-0.694	0.578
ICL	0.984	67	0.533	-0.140	0.293	-0.516	0.578
ISL	0.970	67	0.108	0.379	0.293	-0.622	0.578
IHD	0.977	67	0.261	0.376	0.293	-0.404	0.578

5.2 Comparative tests

As the two LH (right and left), two WHS (right and left), two IC (right and left) and IS (right and left) measurements were normally distributed, a paired t-test (Table 5.2.1) was conducted to compare the three pairs of right and left means. Even though the right PNS was normally distributed, it's corresponding measurement, the left PNS, was not normally distributed and therefore could not be compared using this test.

Table 5.2.1: Paired t-test comparing the normally distributed right and left measurements, with p-values indicating that they could be combined

	Paired differences					t	df	P-value (2-tailed)
	Mean	Std. Deviation	Std. Error Mean	95% CI Difference Lower	Upper			
LHR - LHL	0.522	0.314	0.0370	-0.0216	0.126	1.41	71	0.163
WHSR – WHSL	-0.0218	0.347	0.0403	-0.102	0.0586	-0.540	73	0.591
ICR – ICL	-1.02	8.51	1.01	-3.03	0.997	-1.01	70	0.317
ISR - ISL	2.12	13.0	1.51	-0.896	5.13	1.40	73	0.166

A Wilcoxon Signed-Rank test (Table 5.2.2) was conducted to compare the means of the right and left WHC, and the right and left PNS measurements, which were not normally distributed.

Table 5.2.2: Wilcoxon Signed-Rank test comparing the left and right measurements that were not normally distributed, with p-values indicating that the measurements could be combined

	Z	Assumed p-value (2-tailed)
WHCL - WHCR	-1.35[a]	0.177
PNSL - PNSR	-1.28[b]	0.202

a. Based on negative ranks.

b. Based on positive ranks.

As all the p-values for the paired t-test were above 0.05, they could be combined with each other, yielding a larger sample. Once again, all measurements for the Wilcoxon Signed-Rank test had p-values above 0.05 and could therefore be combined to yield a larger sample. Descriptive statistics (Table 5.2.3) were then made to combine all these pairs.

Table 5.2.3: Descriptive statistical analysis of combined right and left measurements

	N	Mean		Std. deviation	95% CI for mean		Min.	Max.	Range
		Statistic	Std. error		Lower	Upper			
LH	145	2.54	0.0401	0.482	2.46	2.68	1.60	3.76	2.16
WHC	145	1.05	0.0189	0.228	0.982	1.08	0.800	1.80	1.00
WHS	148	1.80	0.0346	0.421	1.67	1.86	0.820	2.91	2.09
PNS	148	11.2	0.143	1.73	10.8	11.6	7.78	15.2	7.46
IC	145	108	0.836	10.1	105	110	82.3	131	48.9
IS	148	87.9	1.60	19.4	84.3	93.8	40.6	137	96.7
IHD	74	16.9	0.356	3.06	16.0	17.5	11.0	24.2	13.2

Key	Description
LH	Length of the pterygoid hamulus
WHC	Width of the pterygoid hamulus in the coronal plane
WHS	Width of the pterygoid hamulus in the sagittal plane
PNS	Distance from the most inferior tip of the pterygoid hamulus to the posterior nasal spine
IC	Inclination of the pterygoid hamulus in the coronal plane
IS	Inclination of the pterygoid hamulus in the sagittal plane
IHD	Pterygoid inter-hamulus distance

The length of the pterygoid hamulus (LH) was shown to be 2.54±0.482mm. The width of the pterygoid hamulus in the coronal plane (WHC) in the sample was 1.05±0.228mm and the width of the pterygoid hamulus in the sagittal plane (WHS) was 1.80±0.421mm. The distance from the most inferior tip of the pterygoid hamulus to the posterior nasal spine (PNS) was found to be 11.2±1.73mm.

The inclination of the pterygoid hamulus is the coronal plane (IC) in this sample was 108±10.1°, and the inclination of the pterygoid hamulus in the sagittal plane (IS) was 87.9±19.4°. Lastly, the inter-hamulus distance (IHD) was found to be 16.9±3.06mm.

5.3 Correlation tests

Correlation between the variables was investigated in order to establish if dependent variables can be extrapolated from independent variables or other dependent variables using the given regression formulas.

To test the strength of correlation between different pairs of variables, a Pearson's correlation test was conducted (Appendix A.4), instead of a Spearman's correlation test since the measurements were linear (taken from an interval scale) as opposed to non-linear (taken from an ordinal scale). Table 5.3.1 illustrates the correlation pairs with an excellent correlation (r>0.7). P-values lower than 0.05 indicates that a regression analysis could be performed.

Table 5.3.1: Correlation coefficient between notable correlation pairs for combined data

Correlation pair	N	Pearson's correlation coefficient (r)	P-value (2-tailed)
Height and PNS	144	0.784	0.000
Height and IHD	72	0.734	0.000
Weight and PNS	148	0.804	0.000
Weight and IHD	74	0.765	0.000
PNS and IHD	74	0.936	0.000

The strong correlation pairs were height and distance from the tip of the hamulus to the posterior nasal spine (PNS), height and inter-hamulus distance (IHD), weight and PNS, weight and IHD, and PNS and IHD.

5.4 Regression analysis

Regression analyses (Table 5.4.1) were conducted between the correlation pairs, with the p-values less than 0.05 indicating that the regression analyses were significant, and a regression formula could be produced. Visual representation of these regressions analyses and formulas are illustrated in appendix A.5-A.9.

Table 5.4.1: Regression analyses between correlation pairs for combined data

Dependent variable	Model	Unstandardised coefficients		P-value	R^2 linear	Std. error of estimate	95% Confidence Interval for B	
		B	Std. Error				Lower	Upper
PNS	Constant	3.68	0.503	0.000	0.614	1.06	2.68	4.67
	Height	18.8	1.25	0.000			16.4	21.3
IHD	Constant	4.49	1.38	0.002	0.539	2.06	1.74	7.25
	Height	31.1	3.44	0.000			24.3	38.0
PNS	Constant	8.55	0.181	0.000	0.644	1.03	8.19	8.91
	Weight	1.79	0.109	0.000			1.57	2.00
IHD	Constant	12.5	0.493	0.000	0.579	1.99	11.5	13.5
	Weight	2.99	0.297	0.000			2.40	3.58
PNS	Constant	2.44	0.394	0.000	0.875	0.601	1.65	3.22
	IHD	0.520	0.0230	0.000			0.474	0.565

For the regression formulas, in the represented figure for each correlation pair (Appendix A.5-A.9), the individual measurements are represented as circles. The mean is represented as the solid line, and the dotted line indicates a 95% confidence interval. The regression formula is found on the figure, either in the upper right corner or the bottom left corner.

5.5 Difference in weight

To determine whether the weight of a neonate makes a difference in the various measurements of the pterygoid hamulus taken, equal variance between the

compared weight populations must first be assumed. The weight populations are categorized as less than or equal to 1kg (W0) or more than 1kg (W1). This weight was chosen as the distinguishing weight as some of the cadavers were observed to be almost half the size of others.

Table 5.5.1 illustrates the frequency in which these two weight populations were found in the sample. In order to compare the means of the two populations using an independent sample t-test, equal variance needs to be assumed. Levene's test for the equality of variances (Table 5.5.2) assesses this assumption.

Table 5.5.1: Frequency table indicating the frequency with which neonates were classified as W0 and W1

	Frequency	Percent
W0	60	40.5
W1	88	59.5
Total	148	100.0

Table 5.5.2: Levene's test for equality of variances, assessing the assumption of equal variance for the population W0 and W1, with p-values lower than 0.05 highlighted

	Levene's test for equality of variances	
	F	**P-value**
LH	1.56	0.213
WHC	5.43	0.0210
WHS	0.867	0.353
PNS	23.7	0.000
IC	0.226	0.635
IS	1.44	0.233
IHD	11.2	0.001

A p-value of less than 0.05 indicates that equal variance cannot be assumed. The length of the pterygoid hamulus (LH), width of the pterygoid hamulus in the sagittal plane (WHS) and inclination of the pterygoid hamulus in the coronal (IC) and sagittal (IS) planes had equal variances. Width of the pterygoid hamulus in the coronal plane (WHC), distance from the most inferior tip of the pterygoid hamulus to the posterior nasal spine (PNS) and the inter-hamulus distance (IHD) did not have equal variances.

An independent sample t-test (Table 5.5.3) was then conducted to determine whether the means of the two populations are equal.

Table 5.5.3: Independent sample t-test for equality of means for W0 and W1. P-value higher than 0.05 is highlighted

	T-test for equality of means						
	t	df	P-value (2-tailed)	Mean Difference	Std. Error Difference	95% CI of the Difference	
						Lower	Upper
LH equal variance assumed	7.23	143	0.000	0.506	0.0700	0.368	0.645
WHC equal variance not assumed	5.45	137	0.000	0.160	0.0352	0.905	0.230
WHS equal variance assumed	2.76	146	0.007	0.190	0.0689	0.541	0.327
PNS equal variance not assumed	12.4	142	0.000	2.40	0.194	2.01	2.78
IC equal variance assumed	3.19	143	0.002	5.27	1.65	2.01	8.53
IS equal variance assumed	0.675	146	0.501	2.20	3.26	-4.24	8.65
IHD equal variance not assumed	8.16	70.2	0.000	4.07	0.500	3.07	5.07

A p-value of less than 0.05 for a t-test for equality of means indicates that, whether equal variance was assumed or not, there is a significant difference between the means of W0 *vs* W1.

The means for all the variables, except inclination of the pterygoid hamulus in the sagittal plane (IS), showed that there is significant difference between the two weight populations. Since the means for IS did not show any significant difference between the two weight populations, the mean from the descriptive statistics performed on the combined left and right sides (Table 5.2.3) can be used.

Table 5.5.4: Descriptive statistical analysis for W0

	N	Mean		Std. deviation	Min.	Max.	Range
		Statistic	Std. Error				
LH	60	2.23	0.0486	0.377	1.61	3.21	1.60
WHC	60	0.938	0.0209	0.162	0.800	1.41	0.610
WHS	60	1.68	0.0481	0.373	1.00	2.61	1.61
PNS	60	9.74	0.110	0.853	7.78	11.5	3.72
IC	59	105	1.32	10.1	82.3	131	48.9
IHD	30	14.5	0.284	1.56	11.0	17.6	6.60

Since there was a difference between the two populations concerning weight, the descriptive statistics were separated (Table 5.5.4 and table 5.5.5). For the population that weighed less than or equal to 1 kg, LH was established to be 2.23±0.377mm, WHC was 0.938±0.162mm and WHS was found to be 1.68±0.373mm. PNS was found to be 9.74±0.853mm. IC was established as 105±10.1°. IHD was found to be 14.5±1.56mm (Table 5.5.4).

Table 5.5.5: Descriptive statistical analysis for W1

	N	Mean		Std. deviation	Min.	Max.	Range
		Statistic	Std. Error				
LH	86	2.74	0.0472	0.438	1.60	3.76	2.16
WHC	85	1.12	0.0245	0.226	0.800	1.61	0.810
WHS	88	1.87	0.0476	0.446	0.82	2.91	2.09
PNS	88	12.1	0.159	1.50	9.06	15.2	6.18
IC	86	110	1.03	9.52	88.3	129	41.0
IHD	44	18.5	0.411	2.72	12.6	24.2	11.6

For the population that weighed more than 1 kg the following means were established: LH was found to be 2.74±0.438mm, WHC was found to be 1.12±0.226mm and WHS was found to be 1.87±0.446mm. PNS in this sample was 12.1±1.5mm. The angle of IC was established as 110±9.52°. IHD was measured as 18.5±2.72mm (Table 5.5.5).

In order to establish whether there was any correlation between different pairs of variables for the population weighing less or equal to 1kg (W0), a Pearson's correlation test was conducted (Appendix B.1). For the W0 sample, the only correlation pair was between PNS and IHD. The sample size for this correlation pair was 30 with a Pearson's correlation coefficient (r) of 0.773 and a P-value (2-tailed) of less than 0.000. A Pearson's correlation coefficient larger than 0.7 indicated and

excellent correlation and a P-value lower than 0.05 indicates that a regression analysis can be made.

A regression analysis (Table 5.5.6) was made for the correlation pair, with the p-value less than 0.05 indicating that the regression analysis was significant and a regression formula could be made. Visual representation of this regression analysis and formula is illustrated in appendix B.3.

Table 5.5.6: Regression analysis between the correlation pair for the W0 sample

Dependent variable	Model	Unstandardised coefficients		P-value	R^2 linear	Std. error of estimate	95% confidence interval for B	
		B	Std. Error				Lower	Upper
PNS	Constant	3.61	0.971	0.001	0.597	0.559	1.62	5.60
	IHD	0.430	0.0670	0.000			0.293	0.566

The same procedure was done for the population weighing more than 1kg (W1). A Pearson's correlation test was conducted (Appendix B.2). For the W1 sample, the only correlation pair was between PNS and IHD with a sample size of 44. The Pearson's correlation coefficient (r) for this pair was 0.912, indicating an excellent correlation. The P-value was found to be less than 0.00, allowing for the creation of a regression analysis.

A regression analysis (Table 5.5.7) was made for the correlation pair, with the p-value less than 0.05 indicating that the regression analysis was significant, and a regression formula could be made. Visual representation of this regression analysis and formula is illustrated in appendix B.4.

Table 5.5.7: Regression analysis between the correlation pair for the W1 sample

Dependent variable	Model	Unstandardised coefficients		P-value	R^2 linear	Std. error of estimate	95% confidence interval for B	
		B	Std. Error				Lower	Upper
PNS	Constant	3.06	0.639	0.000	0.831	0.609	1.77	4.35
	IHD	0.491	0.0340	0.000			0.422	0.560

For the regression formulas, in the represented figures (Appendices B.3 and B.4) for each correlation pair, the individual measurements are represented as circles. The mean is represented as the solid line, and the dotted line indicates a 95% confidence interval. The regression formula is found on the top right corner of the figure.

5.6 Difference in population groups

To determine whether the population group of a neonate makes a difference in the various measurements taken of the pterygoid hamulus, equal variance between the compared population groups must first be assumed. The population groups are categorized as white (WA) or black (BB). Levene's test for the equality of variances (Table 5.6.2) assesses this assumption. Table 5.6.1 illustrates the frequency in which these two populations were found in the sample.

Table 5.6.1: Frequency table indicating the frequency with which neonates were classified as WA and BB

	Frequency	Percent
WA	36	24.3
BB	112	75.7
Total	148	100

A p-value of less than 0.05 indicates that equal variance cannot be assumed. Equal variance was therefore assumed for the length of the pterygoid hamulus (LH), the width of the pterygoid hamulus in the coronal (WHC) and sagittal (WHS) planes, the distance from the most inferior tip of the pterygoid hamulus to the posterior nasal spine (PNS), the inclination of the pterygoid hamulus in the coronal plane (IC) and the inter-hamulus distance (IHD). Equal variance was not assumed for the inclination of the pterygoid hamulus in the sagittal plane (IS).

Table 5.6.2: Levene's test for equality of variances, assessing the assumption of equal variance between populations WA and BB, with p-values lower than 0.05 highlighted

	Levene's test for equality of variances	
	F	P-value
LH	1.03	0.313
WHC	1.59	0.209
WHS	0.633	0.428
PNS	3.22	0.0750
IC	0.781	0.378
IS	16.4	0.000
IHD	0.531	0.468

An independent sample t-test (Table 5.6.3) was then conducted to determine whether the means of the two populations are equal.

Table 5.6.3: Independent sample t-test for equality of means for WA and BB. P-value lower than 0.05 is highlighted

	T-test for equality of means						
	t	df	P-value (2-tailed)	Mean Difference	Std. Error Difference	95% CI of the Difference	
						Lower	Upper
LH equal variance assumed	2.20	143	0.030	0.201	0.0915	0.0203	0.382
WHC equal variance assumed	1.53	143	0.128	0.0666	0.0435	-0.0195	0.153
WHS equal variance assumed	0.061	146	0.952	0.00490	0.809	-0.155	0.165
PNS equal variance assumed	0.996	146	0.321	0.331	0.332	-0.326	0.987
IC equal variance assumed	0.300	143	0.764	0.588	1.96	-3.29	4.46
IS equal variance not assumed	-0.565	44.8	0.575	-2.62	4.63	-11.9	6.71
IHD equal variance assumed	0.491	72	0.625	0.410	0.834	-1.25	2.07

A p-value of less than 0.05 for a t-test for equality of means indicates that, whether equal variance was assumed or not, there is a significant difference between the means of the white population (WA) *vs*. the black population (BB).

Since there was a difference between the two population groups concerning the mean of the length of the pterygoid hamulus (LH), the descriptive statistics were separated (Table 5.6.4). Accordingly, the mean for LH in the white population was found to be 2.69±0.524mm, and the mean in the black population was found to be 2.48±0.462mm.

Table 5.6.4: Descriptive statistical analysis for the LH measurement of WA and BB

	N	Mean		Std. deviation	Min.	Max.	Range
		Statistic	Std. Error				
WA	36	2.69	0.0973	0.524	1.71	3.61	1.90
BB	110	2.48	0.0440	0.462	1.60	3.76	2.16

In order to establish whether there was any correlation between different pairs of variables, a Pearson's correlation test for the white (WA) population was conducted (Appendix C.1). However, because only the length of the pterygoid hamulus (LH) measurement showed a significant difference between population groups, it is the only measurement that can be considered in the Pearson's correlation test.

The only correlation pair with an excellent correlation (r>0.7) was between LH and PNS for the white population. The sample size consisted of 36, with a Pearson's correlation (r) of 708 and a P-value (2-tailed) of less than 0.000. The p-value lower than 0.05 indicates that a regression analysis can be made.

A regression analysis (Table 5.6.5) was made for the correlation pair with the p-value less than 0.05, indicating that the regression analysis was significant and a regression formula could be made. Visual representation of this regression analysis and formula is illustrated in appendix C.2.

Table 5.6.5: Regression analysis between the correlation pair WA

Dependent variable	Model	Unstandardised coefficients		P-value	R^2 linear	Std. error of estimate	95% confidence interval for B	
		B	Std. Error				Lower	Upper
PNS	**Constant**	4.27	1.25	0.002	0.501	1.41	1.73	6.80
	LH	2.66	0.455	0.00			1.73	3.58

For the regression formula, in the represented figure (Appendix C.2) for the correlation pair, the individual measurements are represented as circles. The mean is represented as the solid line, and the dotted line indicates a 95% confidence interval. The regression formula is found on the top right corner of the figure.

This procedure was repeated for the black (BB) population. The Pearson's correlation test can be found in appendix C.1. However, because only the length of the pterygoid hamulus (LH) measurement showed a significant difference between population groups, it is the only measurement that can be considered in the Pearson's correlation test. The test indicated that there was no significant correlation between LH and any of the other variables for this population group.

5.7 Different frequencies of angles observed

While conducting quantitative measurements of the inclination of the pterygoid hamulus in the sagittal (IS) and coronal (IC) planes, it was observed that, in the IS measurements, some of the angles of inclination were anteriorly inclined and others were posteriorly inclined. In the IC measurement, it was observed that some angles of inclination were angled medially, while others were angled laterally.

The inclination taken in the sagittal plane (IS), as illustrated in table 5.7.1, was found to be either directed anteriorly (IS1) or directed posteriorly (IS0). As right and left were combined, the frequency was noted in this group. Because there was shown to be some differences between weight, less than or equal to 1kg (W0), and more than 1 kg (W1), the frequencies were shown in both. Because there was also a difference noted between population groups, white (WA) and black (BB), the frequencies were shown in both.

Table 5.7.1: Frequency of IS0 (angle ≤ 90°) and IS1 (angle > 90°) observed in the combined data group, the two groups separated by weight, and the two groups separated by their population group

	Combined		W0		W1		WA		BB	
	Freq.	%	Freq.	%	Freq.	%	Freq.	%	Freq.	%
IS0	93	62.8	56	63.6	37	61.7	23	63.9	70	62.5
IS1	55	37.2	32	36.4	23	38.3	13	36.1	42	37.5
Total	148	100.0	88	100.0	60	100.0	36	100.0	112	100.0

The majority of the measurements fell under the IS0 category, meaning that the majority of the angles of inclination of the pterygoid hamulus in the sagittal plane were directed posteriorly. The frequencies observed for each of the population groups showed no significant difference between the populations, with frequencies ranging from 36.1% to 38.3% or 61.7% to 63.9%.

The inclination taken in the coronal plane (IC), as illustrated in table 5.7.2, was found to be either directed medially (IC0) or directed laterally (IC1). The observed frequency within each distinct group as shown in figure 5.7.1 was repeated for the coronal inclinations (Table 5.7.2).

Table 5.7.2: Frequency of IC0 (angle ≤ 90°) and IC1 (angle > 90°) observed in the combined data group, the two groups separated by weight, and the two groups separated by their population group

	Combined		W0		W1		WA		BB	
	Freq.	%	Freq.	%	Freq.	%	Freq.	%	Freq.	%
IC0	5	3.4	2	2.3	3	5	2	5.6	3	2.7
IC1	143	96.6	86	97.7	57	95	34	94.4	109	97.3
Total	148	100.0	88	100.0	60	100.0	36	100.0	112	100.0

The majority of the measurements fell under the IC1 category, meaning that the majority of angles of inclination of the pterygoid hamulus in the coronal plane were directed laterally. The frequencies observed for each of the population groups showed no significant difference between the populations, with frequencies ranging from 2.3% to 5.6 % or 94.4% to 97.7%.

5.8 Intra-observer error

In order to establish if the quantitative measurements taken illustrated agreement with each other as done by the main investigator, a Bland and Altman[24] statistical comparison (Table 5.8.1) was constructed between variables from a select number of neonates that were measured again. For this study, the measurements were repeated twice after the initial measurements were taken for the entire sample.

The two repeated samples of measurements were combined to create a more accurate sample of repeated measurements. The repeated sample measurements were then compared to the original sample measurements using a Bland and Altman statistical comparison test. The descriptive statistics of the difference between the two and the means of the two sample measurements were established for each dependent variable. The graphical representation of the Bland and Altman test (Appendix D.1-D.7) compared the difference in a variable to the mean of that same variable.

Table 5.8.1: Bland and Altman statistics comparison for intra-observer error, all measurements in mm and degrees

	DIFFERENCES							MEANS	
	Mean		CI for Mean		Std.	Limit of agreement		Range	
	Stat	Std. Error	Lower	Upper	Deviation	Lower	Upper	Min	Max
LH	0.153	0.0658	0.017	0.288	0.336	-0.506	0.812	-0.475	0.825
WHC	-0.0464	0.0839	-0.219	0.124	0.428	-0.885	0.792	-1.83	0.4
WHS	0.255	0.0924	0.0652	0.446	0.471	-0.668	1.18	-0.7	1.55
PNS	0.12	0.061	-0.0057	0.246	0.311	-0.490	0.730	-0.49	0.8
IC	-2.4	2.4	-7.34	2.54	12.2	-26.3	21.5	-51	14
IS	-1.98	2.34	-6.81	2.85	12	-25.5	21.5	-25.1	17.4
IHD	-0.108	0.0665	-0.245	0.0289	0.339	-0.772	0.556	-1.21	0.5

The following variables showed a relatively high degree of agreement; the width of the pterygoid hamulus in the coronal plane (WHC), the inclination of the pterygoid hamulus in the coronal plane (IC), and the inter-hamulus distance (IHD). The level of agreement was not as accurate for the width of the pterygoid hamulus in the sagittal plane (WHS) and the distance from the most inferior tip of the pterygoid hamulus to the posterior nasal spine (PNS) measurements. It was definitely less accurate for the length of the pterygoid hamulus (LH) and the inclination of the pterygoid hamulus in

the sagittal plane (IS) measurements. These low levels in accuracy can be due to human error while taking measurements.

5.9 Inter-observer error

An inter-observer error test was conducted to establish how repeatable the measurements that were taken by the two investigators was (Table 5.9.1). The visual representations of the Bland and Altman statistics for each measurement can be found in appendix E (E.1 to E.6). The width of the pterygoid hamulus in the sagittal plane (WHS) for inter-observer error is absent as this measurement was added too late to be repeated by the supervisor.

Table 5.9.1: Bland and Altman statistics comparison for inter-observer error, all measurements in mm and degrees

	DIFFERENCES							MEANS	
	Mean		CI for Mean		Std. Deviation	Limit of repeatability		Range	
	Stat	Std. Error	Lower	Upper		Lower	Upper	Min	Max
LH	0.0330	0.0302	-0.0293	0.0953	0.151	-0.263	0.329	-0.340	0.260
WHC	0.0166	0.0258	-0.0366	0.0698	0.129	-0.236	0.269	-0.200	0.405
PNS	0.0376	0.0237	-0.0113	0.0865	0.118	-0.194	0.269	-0.230	0.245
IC	-2.86	2.16	-7.31	1.60	10.8	-24.0	18.3	-53.2	3.83
IS	-0.0554	0.605	-1.30	1.19	3.02	-5.97	5.86	-4.49	4.72
IHD	-0.0375	0.0237	-0.0865	0.0115	0.119	-0.271	0.196	-0.290	0.145

The inclination of the pterygoid hamulus in the coronal plane (IC) measurement showed an extremely high rate of repeatability but was the only one to do so. The width of the pterygoid hamulus in the coronal plane (WHC) measurement was relatively repeatable, but the length of the pterygoid hamulus (LH), the distance from the most inferior tip of the pterygoid hamulus to the posterior nasal spine (PNS), the inclination of the pterygoid hamulus in the sagittal plane (IS) and the inter-hamulus distance (IHD) measurements indicated a low level of repeatability. Establishing a horizontal plane in order to take the IS measurement is especially subject to the investigators discretion, as illustrated by the extensive scatter of data points in appendix E.5.

6. Discussion

6.1 Descriptive statistics

Based on the data gathered in this study, a database was created for the morphometrics of the pterygoid hamulus in South African neonates. By running the appropriate statistics, no significant difference was found between the right and left sides of the pterygoid hamulus for any of the measurements taken. Therefore, the measurements of the database can be used as a baseline for either side (Table 5.2.3).

6.2 Relationship between variables

In order to help researchers and surgeons with their work, extrapolations of pterygoid hamulus morphometrics from biometrics were established (Appendix A.5-A.9). In this database, the following extrapolations can be made; the distance from the most inferior tip of the pterygoid hamulus to the posterior nasal spine (PNS) can be calculated from both the height (A.5) and weight (A.7) of the neonate. The inter-hamulus distance (IHD) can also be calculated from the height (A.6) and the weight (A.8) of the neonate. Additionally, the distance from the most inferior tip of the pterygoid hamulus to the posterior nasal spine (PNS) can be calculated from the inter-hamulus distance (IHD) as show in appendix A.9.

The calculated confidence intervals (CI) for these extrapolations were all narrow (Table 5.4.1), indicating that there is little room for error. The CI's were as follows; 16.4 to 21.3 for PNS and height, 1.57 to 2.00 for PNS and weight, 24.3 to 38.0 for IHD and height, 2.40 to 3.58 for IHD and weight and 0.474 to 0.565 for PNS and IHD. This will be a repeated theme throughout this study since many of the measurements taken were so small.

6.3 Comparing variables with weight populations

As there was a definite difference in the weight and therefore overall size of the neonate between the majority of the sample, a need existed to investigate whether weight had an effect on the measurements of the variables. The statistical analysis

indicated that there was indeed a significant difference in the measurements based on the weight of the neonate.

The following measurements therefore had to be separated according to weight; the length of the hamulus (LH), the width of the hamulus in both the coronal (WHC) and sagittal (WHS) planes, the distance from the most inferior tip of the pterygoid hamulus to the posterior nasal spine (PNS), the inclination of the pterygoid hamulus in the coronal plane (IC) and the inter-hamulus distance (IHD). However, there was no significant difference observed between different weight classes and the inclination of the pterygoid hamulus in the sagittal plane (IS), this may be due to the fact that the factor that determines the angle of inclination is tensile pull of the muscle, and not size or weight of the neonate.

These findings indicate that weight needs to be considered when determining the morphometrics of the pterygoid hamulus. For this reason, since there was no significance between right and left sides of the hamulus, the descriptive statistics calculated for the different weight classes (Table 5.5.4 and Table 5.5.5) need to be used when calculating morphometrics. The exception is the inclination of the pterygoid hamulus in the sagittal plane (IS), where the descriptive statistics for the combined right and left sides (Table 5.2.3) need to be used.

Furthermore, within these descriptive statistics, there still remains a significant correlation between the distance from the most inferior tip of the hamulus to the posterior nasal spine (PNS) and the inter-hamulus distance (IHD). This correlation may be due to the craniofacial growth pattern in neonates, when the sphenoid bone is developing without the influence of the tensile pull exerted by the muscles attached to the pterygoid hamulus. This indicates that for the PNS measurement, it can still be calculated from the measurement of the IHD within each weight class (Appendix B.3 and B.4).

For the lower weight class, that of the sample weighing less than or equal to 1 kg, an outlier was observed (Appendix B.3). This neonate had a significantly larger inter-hamulus distance, that of 17.6mm compared to the average of 14.5±1.58mm, than could be expected from the correlating measurement of the PNS observed, which

was 9.60mm. For this PNS measurement, the correlating IHD measurements should have been 14.2mm. This could indicate that the same degree of lateral inclination of the pterygoid hamulus (IC1) was observed in this neonate as in the rest of the population, but the hamuli were further apart than what would be expected. The distance between the medial pterygoid plates of the sphenoid bone would therefore be wider than expected, as one would find in congenital growth disturbances.

Another possibility that explains this discrepancy is a significantly shorter pterygoid hamulus compared to the inter-hamulus distance. The latter explanation is more likely, because as previously stated, there is a correlation between PNS and IHD. Therefore, the discrepancy is most likely due to this variable.

6.4 Comparing variables with population groups

The last demographic variable this study investigated, was the population group. No comparison between sexes were made, as there is no sexual dimorphism observed between neonates for the total population of this study, as the amount of hormones responsible for secondary sexual characteristics are not observed in newborns. Additionally, Krmpotić-Nemanić *et al.,*[14] and Orhan *et al.*[15] reported no difference between male and female in their measurements even in adults. As previously mentioned, the only population groups available in this study were white and black populations. In order to interpret the statistics calculated, it is important to note that the sample size was very skewed (112 black neonates and 36 white neonates) where this population group was concerned, with the black population making up roughly three-quarters of the sample.

Length of the pterygoid hamulus (LH) was the only variable that showed a significant difference between the two population groups (Table 5.6.3), indicating that the population group should be considered when this specific morphometric variable is considered. Although a correlation was established between the length of the pterygoid hamulus (LH) and the distance from the most inferior tip of the pterygoid hamulus to the posterior nasal spine (PNS) for the white population, and a regression formula could therefore be calculated, the correlation was just barely significant (Appendix C.1).

The regression formula calculated for the correlation between LH and PNS for the white population may not be accurate considering that the white population only made up a quarter of the population, and the same correlation between LH and PNS for the much larger black population was not significant. This is further confirmed when observing the graph of the regression formula (Appendix C.3), with scattered data points and a much larger than normally observed confidence interval (CI). This regression formula therefore should be used with caution.

6.5 Observations of the frequencies of the angles of inclination

Although the observations of the frequencies of the angles of inclination was largely a quantitative measurement in this study, it was also a qualitative variable. In order to establish if the anatomy observed in the South African neonatal population corresponded to the anatomy found in modern literature,[6,13] the angles of inclination were noted as either lateral (IC1) or medial (IC0) in the coronal plane, or anterior (IS1) and posterior (IS0) in the sagittal plane.

According to the available literature, the observed inclination of the pterygoid hamulus is lateral in the coronal plane, and posterior in the sagittal plane.[13] This was corroborated by the results found in this study, with the angles of inclination occurring in the same frequency no matter what population group it was divided into (right *vs*. left, less than or equal to 1kg *vs*. more than 1kg, black *vs*. white) as observed in table 5.7.1 and table 5.7.2.

Although a medially inclined pterygoid hamulus was less common, it still occurred in 2.3% to 5.6% of the population. Anteriorly inclined hamuli were found more frequently, in 36.1% to 38.3% of the population, than would be observed in adults according to the literature.[6,13] These discrepancies can be due to the fact that tensile pull from the attached muscles have not yet inclined the hamuli in the normally observed directions. It is therefore an important observation to keep in mind when surgeons are working on neonates.

6.6 Comparing results to other studies

Although the quantitative measurements for this study could not accurately be compared to those of the reference studies because of various reasons that will be discussed during the limitations section (section 6.8), a table was drawn up to show the results of all the studies (Table 6.6.1). The main reason the measurements cannot be compared is the difference in age between the reference studies and the current study. The reason being that the pterygoid hamulus changes in shape and size as age increases.

As shown in the table below, some measurements were omitted by the different researchers, limiting comparison further. Some of these studies did not specify the exact way in which measurements were taken, making exact repeatability difficult. Furthermore, these studies used skulls instead of CBCT scans for quantitative data collection. Since the pterygoid hamulus is such a delicate structure, the maceration process can severely damage it especially in neonates, making the measurements inaccurate. For this reason macerated neonate skulls were not measured in this study.

In order to compare measurements in previous studies to the measurements in this study, specific age subgroups as stated by the authors were chosen. These age groups will be discussed in the following paragraphs in order to compare the results in table 6.6.1.

Putz and Kroyer[13] did not divide their sample into age groups, therefore the measurements in table 6.6.1 are the collective measurements for all ages. 20.5% of their sample consisted of children's skulls. Krmpotić-Nemanić *et al*.[14] used skulls of various ages as well, but divided their sample into three groups; children, adults and elderly. The measurements used in table 6.6.1 came from the children's group. This category ranged from the ages of new-born to nine years old, and consisted of 47.7% of their sample.

The sample of Orhan *et al.*[15] ranged in age from 22 to 75 years and was divided into two groups; 22 to 55 years and older than 55 years. The data in table 6.6.1 is from

the younger group. Raijon *et al.*[16] conducted their study on a population with ages ranging from zero to 12 months. Their population was subdivided into infants that had non-cleft palates and those that did. The non-cleft category made up 29.3% of their sample, the measurements in table 6.6.1 were taken from this group.

Table 6.6.1: Summary of all the quantitative measurements for all the studies related to the morphometry of the pterygoid hamulus

	Current study (2020)	Putz and Kroyer[13]	Krmpotić-Nemanić *et al.*[14]	Orhan *et al.*[15]	Rajion *et al.*[16]
LH (mm)	2.54 ± 0.482	7.2	3.6 ± 1.5	6.38 ± 1.93	-
WHC (mm)	1.05 ± 0.228	2.3	-	1.85 ± 0.88	-
WHS (mm)	1.80 ± 0.421	1.4	-	-	-
PNS (mm)	11.2 ± 1.73	-	-	21.73 ± 2.54	-
IC (degrees)	108 ± 10.1	122	-	126.1 ± 2.18	-
IS (degrees)	87.9 ±19.4	75	19.6 ± 12.1	82.8 ± 2.99	-
IHD (mm)	16.9 ± 3.06	26-36.9	31.0 ± 3.7	-	25.6 ± 0.77

By comparing this study's measurements with those made by other studies with similar age groups (Krmpotić-Nemanić *et al*.[14] and Rajion *et al*.[16]), we can establish the level of agreement between the studies. The length of the pterygoid hamulus (LH) is 70.6% the length of the measurement found by Krmpotić-Nemanić *et al*.[14]

The inclination of the pterygoid hamulus in the sagittal plane (IS) for this study was larger than that found by Krmpotić-Nemanić *et al*.[14] by 24.9%, indicating a more posteriorly directed inclination. This could be due to the muscles not yet exerting a more latero-caudal pull, so that the pterygoid hamulus is still directed mostly posterior. This is further reinforced by the fact that the inclination of the pterygoid hamulus in the coronal plane (IC) is not as large for this study as the angle found in the other studies. This smaller IC implies that the muscles have not yet asserted a lateral pull on the hamulus.

The inter-hamulus distance (IHD) for this study is 54.5% the distance of Krmpotić-Nemanić *et al*.[14] and 66% the distance of the same measurement for Rajion *et al.,*[16] this indicates that the there is a definite difference between the size of the sphenoid

where age is concerned. Comparison of the current study's measurements to those performed containing older samples (Putz and Kroyer[13] and Orhan *et al.*[15]), most measurements are not as large as those found in adults, as would be expected. This might be an indication of how much the neonatal skull grows in the first year.

6.7 Abnormality found

An abnormally shaped pterygoid hamulus structure was observed while conducting quantitative measurements in the coronal plane (Figure 6.7.1). When taking measurements in the sagittal plane (Figure 6.7.2), the abnormality was confirmed as an elongated pterygoid hamulus. The neonate was a white male of height 0.32m and weight 0.8kg.

Even though an abnormality was detected, the quantitative measurements of this scan had no outliers. The clinical implications of an elongated hamulus that would have been experienced are discussed in the Pathology section of the Literature review, these mainly relate to misdiagnosis due to the generalized location of pain.[9,20-21]

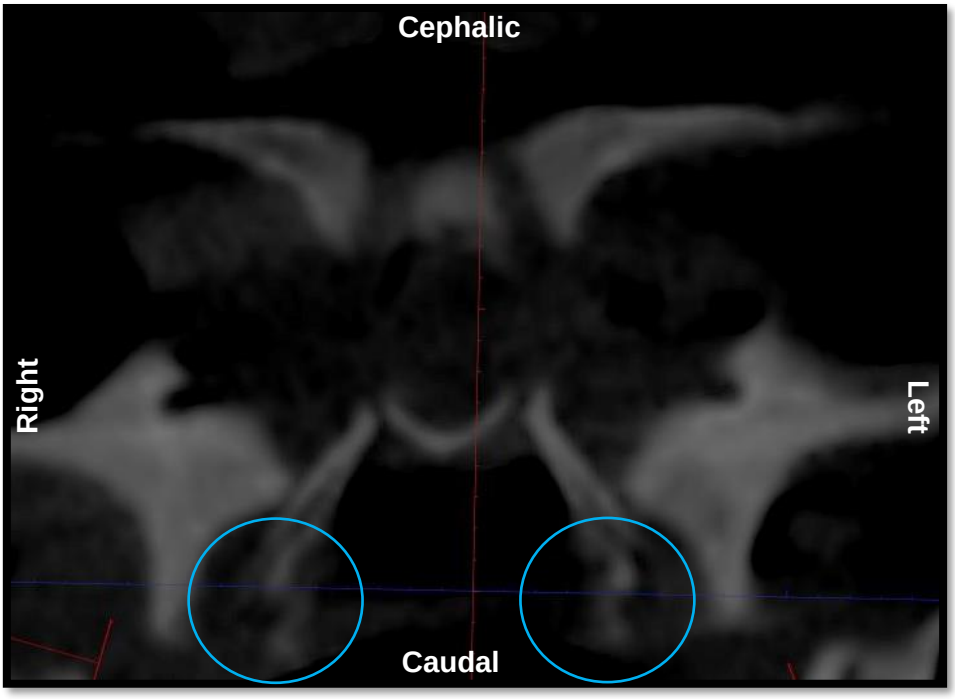

Figure 6.7.1: CBCT scan in the coronal plane of a neonatal sphenoid indicating the pterygoid hamuli. The blue circles indicate the abnormality first observed in the coronal plane.

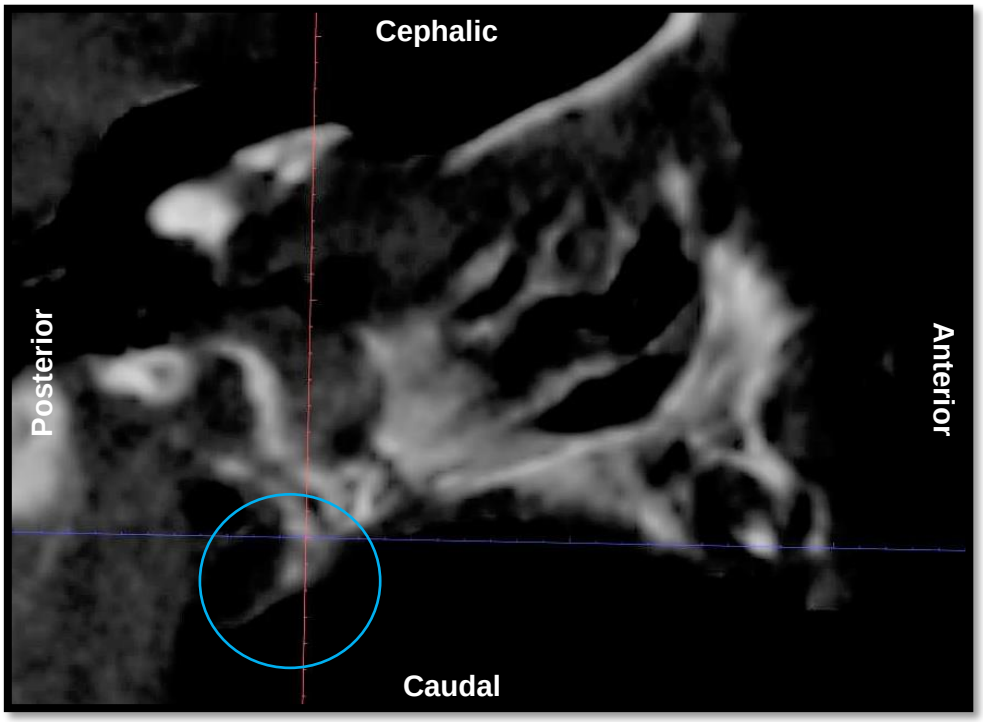

Figure 6.7.2: CBCT scan in the sagittal plane of a neonatal skull indicating the pterygoid hamulus. The blue circle indicates the elongated hamulus.

6.8 Limitations of the study

The low weight of the neonates available to the university is a major limitation as the reparative surgery is usually done at five months of age when the weight is approximately between 6 and 7 kg as opposed to the average of roughly 1.5-2.5 kg for the neonates available.

It was discovered during collection of qualitative measurements that the Planmeca Romexis 4.6.0.R program only measured a minimum of 0.8mm and therefore any results smaller than this were noted as equal to or less than the minimum. Not all South African population groups are represented in this study as the cadavers were sourced from Gauteng. Only white and black neonatal cadavers were available to the University of Pretoria.

Interpretation of which sagittal section to use in order to measure the angle of inclination of the pterygoid hamulus in the sagittal plane was subjective, therefore the angle may differ between observers. The main investigator in this study used the sagittal section in the sagittal plane that showed the most complete section of the pterygoid hamulus.

The available references used for comparison to this study all use various different techniques during collection of qualitative data without exactly specifying their methodology. Specifically the establishment of a standardised horizontal plane was often poorly explained which resulted in problems with the repeatability of their methods.

Another limitation is that this study could not be compared with the references used as they mostly had a sample of adults, and if children were present in the sample, they were either older than the specified 28 days for neonates, or were not classified into age groups. Lastly, because the WHS measurement was not repeated by the supervisor in order to complete an inter-observer error test, the repeatability of this measurement could not be established or compared to the intra-observer error test for the same measurement.

7. Conclusion

The pterygoid hamulus is an important structure when considering the functionalities of the muscles attached to it, especially the tensor veli palatini, and by proxy, the Eustachian tube. Knowing the shape, size, position and inclination of the pterygoid hamulus is important when surgeries are performed in the surrounding area. As it is a structure that changes with time, knowing its morphometrics is important in all age groups, not just in adults, especially since major surgeries such as cleft palate repair is performed in early infancy.

This study established a database for the neonatal pterygoid hamulus morphometrics. Such detailed information has been missing from the literature up until now. The aim of this database was to provide surgeons and researchers with a baseline to start from when considering the pterygoid hamulus itself or perhaps the structures surrounding it. To aid further in this knowledge base, correlations between known demographic independent variables, height and weight, and the unknown dependent morphological variables PNS and IHD were established. A correlation between PNS and IHD was also established. This will allow for possible preoperative determination of the morphology or relationships of the pterygoid hamulus in a South African neonatal population in the absence of advanced scanning methodology.

Weight was found to be an important determining factor when distances between different bony structures of the skull were measured. As weight increases, so does the distance between the most inferior tip of the pterygoid hamulus and the posterior nasal spine (PNS), as well as the inter-hamulus distance (IHD). Height was also observed to have a lesser, but by no means less determining influence on the morphology of the pterygoid hamulus. Height, in the same manner as weight relates to the overall size of a neonate, with a larger neonate having a larger bone structure.

The population group was another demographic variable that was considered in this study when establishing correlations between the measurements taken. However, based on our results, it does not appear to have a determining factor when it comes to the morphology of the pterygoid hamulus.

The inclination of the pterygoid hamulus is an important factor to consider during surgery in the surrounding area. This study found that the inclination of the hamulus agrees with that found in modern literature thus far. The inclination of the pterygoid hamulus is independent of any of the previously mentioned demographic variables, and therefore dependent only on tensile pull of the muscles. It is important to keep in mind however, that due to the young age of the cadavers, the muscles have not had time to exert this pull and therefore the inclination is not as postero-laterally directed as the inclinations that can be found in adults and even older infants.

These morphometrics and the correlations between the morphometrics needs to be kept in mind when considering the pterygoid hamulus and its surrounding area during research or when considering anatomical variations or abnormalities such as an elongated pterygoid hamulus or cleft palate. The importance of knowing the morphometry of the pterygoid hamulus in neonates cannot be overstated, especially when considering how this morphology will change with age, abnormalities or the correction of abnormalities.

8. Future recommendations

As was mentioned earlier, this study was limited in several factors, the least of which was the limited sample size available, despite this being one of the largest studies of its kind. Furthermore, a sparsity exists by way of similar studies with which to compare our results. As time was also a limiting factor, the following recommendations were identified and would add significantly to the data obtained in this study.

Firstly, it will be beneficial to be able to distinguish between the measurement of the length of the pterygoid hamulus in both the coronal and sagittal planes. This might increase the reliability of the measurement, especially in the sagittal plane, as the entirety of the pterygoid hamulus can be observed in this plane, as opposed to the coronal view that displays the pterygoid hamulus as ending at the point where the head angles anteriorly.

In order to have more accurate information on the length of the pterygoid hamulus when comparing the two population groups studied in this thesis, it is important to compare the results between equal numbers of both samples, or at least a larger sample of white neonates.

Building on this study, a database of the morphology of the pterygoid hamulus in neonates with cleft palates should be established. This will allow for comparison of the two databases in order to establish exactly how a cleft palate affects the anatomy of the pterygoid hamulus, and therefore the tensor veli palatini and the Eustachian tube. This cleft-palate database can further be used to assess and improve on Prof. Bütow's tensor sling procedure[23] for the corrective surgery of cleft palates.

Lastly, by using micro-CT scans, more accurate measurements can be obtained as the measuring process is more precise with 27.2µm voxel size as compared to CBCT with 200µm, leading to greater image spatial resolution.[25] However, micro-CT scans are very expensive and it takes a considerably longer time to take the scans. Thus, a study to compare the accuracy of both scanning methods could be conducted as a proof of concept.

9. References

1. Kronman JH, Padamsee M, Norris LH. Bursitis of the tensor veli palatini muscle with an osteophyte on the pterygoid hamulus. Oral surgery, oral medicine, oral pathology. 1991 Apr;71(4):420-2.
2. Blumen MB, Dahan S, Fleury B, Hausser-Hauw C, Chabolle F. Radiofrequency ablation for the treatment of mild to moderate obstructive sleep apnea. The Laryngoscope. 2002 Nov;112(11):2086-92.
3. Cahali MB. Lateral pharyngoplasty: a new treatment for obstructive sleep apnea hypopnea syndrome. The Laryngoscope. 2003 Nov;113(11):1961-8.
4. Roode G, Bütow K-W. Pterygoid Hamulus Syndrome-Undiagnosed. The South African Dental Journal. 2014 Mar; 69(2):70-71.
5. Laifer-Narin S, Schlechtweg K, Lee J, Booker W, Miller R, Ayyala RS, Imahiyerobo T. A comparison of early versus late prenatal magnetic resonance imaging in the diagnosis of cleft palate. Annals of plastic surgery. 2019 Apr;82(4S):S242-6.
6. Standring S, Anand N, Birch R, Collins P, Crossman AR, Gleeson M. *et al.* Gray's anatomy: the anatomical basis of clinical practice. 41st ed. Edinburgh: Churchill Livingstone/Elsevier; 2016. p. 495, 571-585.
7. Hertz RS. Pain resulting from elongated pterygoid hamulus: report of case. Journal of oral surgery. 1968 Mar;26(3):209.
8. Eyrich GK, Locher MC, Warnke T, Sailer HF. The pterygoid hamulus as a pain-inducing factor: a report of a case and a radiographic study. International journal of oral and maxillofacial surgery. 1997 Aug;26(4):275-7.
9. Sasaki T, Imai Y, Fujibayashi T. A case of elongated pterygoid hamulus syndrome. Oral diseases. 2001 Mar;7(2):131-3.
10. Cole RM, Cole JE, Intaraprasong S. Eustachian tube function in cleft lip and palate patients. Archives of Otolaryngology. 1974 May;99(5):337-41.
11. Paradise JL. Middle Ear Problems Associated with Cleft Palate: An Internationally-oritented review. The Cleft palate journal. 1975 Jan;12(1):17-22.
12. Shankland II WE. Pterygoid hamulus bursitis: one cause of craniofacial pain. The Journal of prosthetic dentistry. 1996 Feb;75(2):205-10.
13. Putz R, Kroyer A. Functional morphology of the pterygoid hamulus. Annals of anatomy= Anatomischer Anzeiger: official organ of the Anatomische Gesellschaft. 1999 Jan;181(1):85-8.

14. Krmpotić-Nemanić J, Vinter I, Marušić A. Relations of the pterygoid hamulus and hard palate in children and adults: anatomical implications for the function of the soft palate. Annals of Anatomy-Anatomischer Anzeiger. 2006 Jan 3;188(1):69-74.
15. Orhan K, Sakul BU, Oz U, Bilecenoglu B. Evaluation of the pterygoid hamulus morphology using cone beam computed tomography. Oral Surgery, Oral Medicine, Oral Pathology, Oral Radiology, and Endodontology. 2011 Aug;112(2):e48-55.
16. Rajion ZA, Al-Khatib AR, Netherway DJ, Townsend GC, Anderson PJ, McLean NR. The nasopharynx in infants with cleft lip and palate. International journal of pediatric otorhinolaryngology. 2012 Feb;76(2):227-34.
17. Sadler TW. Langman's Medical Embryology. 13th ed. Philadelphia: Wolters Kluwer; 2015. p. 297.
18. Marieb EN, Hoehn K. Human Anatomy & Physiology. 9th ed. Boston: Pearson; 2013. p. 330-337
19. Shetty SS, Shetty P, Shah PK, Nambiar J, Agarwal N. Pterygoid Hamular Bursitis: A Possible Link to Craniofacial Pain. Case reports in surgery. 2018;2018.
20. Gores RJ. Pain due to long hamular process in the edentulous patient. Report of two cases. The Journal-Lancet. 1964 Oct;84:353.
21. Naidoo S *et al.* 2014. Palatal pain due to exostosis of the posterior palatal spine in a cleft patient. Journal of Cleft Lip Palate and Craniofacial Anomalies. 2014 1: 124-126.
22. Agrawal K. Cleft palate repair and variation. Indian journal of plastic surgery. 2009 Oct;42(Suppl):S102-S109
23. Bütow K-W, Zwahlen R. Cleft ultimate treatment. 2nd Ed. p. 200-3.
24. Bland JM, Altman DG. Statistical methods for assessing agreement between two methods of clinical measurement. International journal of nursing studies. 2010 Aug;47(8):931-936
25. Taylor TT, Gans SI, Jones EM, Firestone AR, Johnston WM, Kim DG. Comparison of micro-CT and cone beam CT-based assessments for relative difference of grey level distribution in a human mandible. Dentomaxillofacial Radiology. 2013 Mar;42(3):25117764.

Appendix A

A.1: Data collection sheet for measurements made, with all distances and lengths (right and left LH, WHC, WHS, PNS and the singular IHD) measured in millimetres, and all angles (right and left IC and IS) measured in degrees. Outliers are highlighted

CADAVER #	LHR	WHCR	WHSR	PNSR	ICR	ISR	LHL	WHCL	WHSL	PNSL	ICL	ISL	IHD
4373	2.79	1.26	2.41	12.19	111.04	123.69	3.06	1.41	2	12.45	105.9	116.57	17.8
4721	3.21	1.2	2.06	9.22	93.58	61.51	3.03	1.4	1.52	9.76	100.61	72.28	12.61
5085	2.51	0.82	2.21	13.24	124.34	56.31	2.72	1	2.47	12.93	125	63.43	20.61
5257	3.23	1.22	1.8	14.04	118.3	89.99	2.72	1.02	2.01	14.59	127.06	80.54	22.6
5258	2.47	1	2.21	11.33	106.52	93.94	2.2	1.22	2.01	10.12	83.66	63.56	14.83
5266	3.33	1	2.21	13.29	122.73	118.62	2.79	1.2	2.2	13.02	109.65	105.25	18.4
5395	3.4	1.41	1.61	14.56	118.07	131.99	3.12	1.17	1.44	15.16	129.29	124.99	24.24
5410	3.16	1	1.4	13.37	109.65	107.1	3.1	1.41	1.8	13.96	104.03	100.3	21
5411	2.47	1.22	1.8	11.35	102.99	108.43	2.86	1.6	2	11.81	102.09	95.2	17.8
5427	2.28	0.82	1.4	8.4	104.03	63.44	1.71	0.8	1.46	8.49	104.05	63.43	11
5436	2.61	1.41	1.81	12.74	120.26	60.25	2.78	1.02	2.28	13.31	120.26	75.96	19.02
5606	2.41	1.02	1.61	10.05	88.33	70.91	1.9	1.02	1.61	9.06	68.7	40.61	14.05
5699	1.8	0.8	1.22	7.96	92.38	74.99	1.81	1	1.02	8.49	94.04	78.49	11.21
5843	2.72	0.82	1.84	10.35	103	90	2.34	1.02	2.01	10.76	104.04	84.81	16.21
5859	2.86	0.82	2.2	12.03	102.1	90.01	2.85	1.02	2.21	12.04	104.04	63.43	18.01
5936	2.95	0.82	1.26	11.46	115.7	115.17	2.24	0.8	1.61	10.91	118.02	122.7	15.6
5937	2.61	0.82	1.79	11.93	124.86	131.19	2.61	0.89	1.79	11.44	122.47	131.19	19.2
5941	2.78	1.22	1.84	14.21	120.25	137.29	3.4	1	1.97	14.32	119.36	128.55	21.4
5945	1.84	1	1.8	9.96	102.53	116.57	1.84	0.8	2.24	9.48	104.03	75.96	14.81
6051	2.86	1.02	2.6	11.78	102.09	75.96	2.67	1	2.2	11.32	102.99	85.23	17.2
6077	3.05	1.22	1.81	12.74	113.2	101.31	3.44	1.41	2.24	13.45	122.74	100.3	20
6138	2.51	1.08	2.04	13.48	120.96	90.01	2.6	1.02	2.21	12.73	116.23	78.69	20.6
6149	2.83	2.83	2.04	10.81	94.08	73.67	3.13	1	1.46	11.6	115.27	71.2	18.04
6151	2.72	1.22	1.27	9.78	107.11	101.31	2.72	1.08	1.2	8.91	102.98	90	14.6
6154	3.22	1.4	1.4	9.76	97.11	89.99	3.21	1.61	2.01	9.35	96.72	90	13.2
6193	2.72	1.02	1.81	10.63	107.11	62.99	2.61	1.2	1.61	10.76	98.12	82.27	16.03
6279	1.79	1	1.52	10.32	116.58	110.55	2.09	1.02	1.4	10.33	106.7	105.94	14.2
6478	2.15	0.82	2.34	10.56	116.57	66.04	2.34	0.89	2.4	10.2	114.45	78.69	16
6502	3.05	1.22	1.84	12.59	118.31	106.7	3.23	1.26	1.61	13.1	121.61	116.57	19.6
6583	2.78	1.22	1.4	12.61	120.26	90	2.78	1.26	1.22	13.32	118.31	89.99	21.8
6589	4.24	1.84	2.21	14.56	110.22	84.29	4.37	1.26	2.81	14.02	105.94	80.54	22.4
6607	2.86	1.02	2.21	13.02	101.31	78.01	2.72	1.02	2.91	12.87	113.44	70.02	19
6608	2.24	0.82	2.01	9.81	101.3	116.57	2.33	0.89	1.6	10.07	122.47	101.3	15
6609	2.86	0.89	1.81	12.16	113.2	83.66	2.68	0.85	2	11.76	116.57	83.66	18.41
6618	3.76	1.08	2.63	13.93	116.56	80.54	3.23	1.02	2.61	13.31	118.07	85.6	20.82
6620	2.28	0.82	1	10	106.71	89.67	2.15	0.82	1.2	10.05	119.16	85.17	15.62
6621	3.3	0.82	2	13.02	103.24	86.56	3.3	1.02	1.8	12.74	105.52	86.53	17.8
6622	2.24	0.82	1.22	10.2	100.3	102.53	2.04	0.8	1.22	10.48	100.31	101.32	15.4
6629	2.61	0.82	1.81	9.6	124.99	72.81	2.13	0.82	1.2	10.65	138.81	64.74	17.6
6631	2.13	0.89	1.81	11.24	131.18	90.01	2.88	0.82	1.61	10.48	122.47	88.46	17.22
6632	2.26	0.89	2.6	13.33	135	73.64	2.24	1.22	1.9	12.21	103.32	92.29	22.02
6633	1.84	0.8	1.8	9.96	102.52	116.57	1.8	0.82	2.2	9.06	90.01	108.43	14.4
6636	2.09	0.8	1.41	9.09	106.69	59.02	2.04	0.8	1.65	9.22	101.31	66.79	14.2
6656	2.2	0.8	1.6	10.04	90.01	90	2.09	0.82	1.4	9.48	109.98	89.99	14.41
6659	2.34	1.02	1.08	8.34	108.44	113.35	2.09	1	1.26	7.78	111.03	112.27	11.8
6682	2.34	1.6	1.34	12.65	109.99	129.89	2.24	1.4	2.01	13.16	116.57	105.95	21.4

6925	1.71	1.02	1.41	9.35	110.56	98.12	1.89	0.82	1.08	9.76	123.69	81.29	13.4
6691	2.28	1.2	2.28	10.19	105.26	108.43	1.71	1.41	2.61	10.28	109.32	113.2	15.61
6744	2.86	1.4	1.8	10.37	102.09	59.74	3.01	1.4	1.4	10.28	93.81	56.31	17.2
6817	2	1.41	1.9	9.9	90	90.01	1.81	1	1.65	9.77	96.34	96.34	13.2
6819	3.23	1.2	2.24	12.76	111.8	90	3.49	1.4	1.81	13.37	113.63	115.09	19.6
6853	2.21	1.22	1.61	9.92	96.33	69.45	1.79	1	2.01	9.96	113.2	74.06	15.01
6880	2.04	1	2.09	12.19	101.31	100.3	1.6	1.02	2.2	10.75	91.23	82.88	16.61
6908	2.28	1.4	2.61	13.62	105.25	105.26	2.24	1.6	2.83	14	116.57	115.08	21.6
6903	2.6	1.4	2.01	15.24	112.61	90	2.33	2.01	1.41	14.52	120.97	91.25	23.4
6937	1.97	0.8	2.21	9.4	113.95	90	1.61	0.8	2.41	8.22	119.74	101.31	14.2
6938	2.67	1.2	2.21	10.2	102.99	102.53	3.03	1	1.84	9.81	97.59	105.25	14.01
6961	2.43	1.02	1.52	10.91	100.3	80.53	2.63	1	1.46	11.5	100.25	69.44	17.2
7000	2.91	1.02	1.65	10.75	105.94	85.11	2.47	1.02	1.97	10.32	104.03	84.46	15.41
7021	3.35	1.02	1.8	11.63	107.35	73.3	3.61	1.4	1.65	10.19	93.37	53.97	15.81
7027	3.16	1.2	0.82	11.96	109.66	68.2	3.16	0.82	1.41	11.61	108.43	84.81	18.2
7029	1.8	0.8	1.4	8.88	90.01	78.68	2.24	0.8	1	8.68	101.32	74.05	14.2
7062	2	0.8	1.9	8.92	92.87	76.09	2.41	0.8	1.71	9.2	82.28	70.51	13.2
7066	2.41	0.8	1.61	12.93	95.2	70.02	2.61	0.82	1.61	12.46	94.4	65.55	19.4
7093	2.28	1.02	1.41	11.06	104.04	83.66	2.24	1.4	1.6	11.03	99.46	78.68	16.4
7121	2.61	1.22	1.81	9.34	94.76	84.29	2.53	1.02	2.09	10.05	106.71	71.57	14
7177	2.34	1.22	1.4	11.18	111.8	61.72	2.34	1.22	1.02	12.12	112.63	61.67	18
7316	1.9	0.8	1.41	8.63	110.64	74.99	1.9	0.8	1.4	8.5	108.31	61.49	12.82
7354	2.53	0.82	1.81	10.53	109.98	96.35	2.04	1	2.01	10.05	102.52	98.13	14.8
7365	2.47	1	1.81	10.35	104.04	71.56	2.09	1	1.81	10.53	108.43	83.66	16.02
7427	3.21	0.8	1.65	10.48	93.81	66.04	2.61	0.8	2.01	10.28	95.19	74.74	15.83
7515	2.28	1.02	1.4	10.76	105.26	73.29	2.47	1	2.21	10.47	104.04	74.05	15
7535	2.21	0.8	1.84	10.5	97.26	89.2	2.53	0.8	1.41	9.78	109	77.84	15.4
7579	2.6	0.8	1.4	10.53	117.17	66.21	2.79	0.8	1.5	10.33	108.87	107.62	15.81

A.2: Descriptive statistical analysis of all measurements before they were standardised, measured in millimetres

	N	Mean	Std. Error	Std. deviation	Min.	Max.	Range
LHR	74	2.58	0.0581	0.500	1.71	4.24	2.53
WHCR	74	1.07	0.0359	0.308	0.800	2.83	2.03
WHSR	74	1.79	0.0458	0.394	0.82	2.63	1.81
PNSR	74	11.2	0.198	1.70	7.96	15.2	7.28
ICR	74	108	1.18	10.2	88.3	135	46.7
ISR	74	88.9	2.30	19.8	56.3	137	81.0
LHL	74	2.53	0.0636	0.547	1.60	4.37	2.77
WHCL	74	1.07	0.0295	0.253	0.800	2.01	1.21
WHSL	74	1.81	0.0522	0.449	1.00	2.91	1.91
PNSL	74	11.1	0.207	1.78	7.78	15.2	7.38
ICL	74	108	1.38	11.9	68.7	139	70.1
ISL	74	86.8	2.22	19.1	40.6	131	90.6
IHD	74	2.58	0.0581	0.500	1.71	4.24	2.53

A.3: Shapiro-Wilk test, Skewness and Kurtosis of unstandardised measurements, with p-values, skewness and kurtosis statistics indicating measurements that could not be compared using a paired t-test (not normally distributed)

	Shapiro-Wilk			Skewness		Kurtosis	
	Mean	df	P-value	Statistic	Std. Error	Statistic	Std. Error
LHR	0.969	74	0.069	0.597	0.279	0.526	0.552
WHCR	0.734	74	0.000	2.88	0.279	13.9	0.552
WHSR	0.975	74	0.153	0.093	0.279	-0.246	0.552
PNSR	0.972	74	0.095	0.333	0.279	-0.690	0.552
ICR	0.984	74	0.484	0.291	0.279	-0.169	0.552
ISR	0.963	74	0.028	0.483	0.279	-0.436	0.552
LHL	0.971	74	0.089	0.543	0.279	0.427	0.552
WHCL	0.864	74	0.000	1.17	0.279	1.47	0.552
WHSL	0.974	74	0.131	0.330	0.279	-0.323	0.552
PNSL	0.962	74	0.024	0.378	0.279	-0.764	0.552
ICL	0.983	74	0.402	-0.340	0.279	0.899	0.552
ISL	0.982	74	0.365	0.292	0.279	-0.319	0.552
IHD	0.973	74	0.108	0.390	0.279	-0.530	0.552

A.4: Pearson's correlation test indicating the strength of correlation between different measurements of combined left and right sides. Green shows excellent correlation, blue shows moderate correlation

		Height	Weight	LH	WHC	WHS	PNS	IC	IS	IHD
Height	Pearson's correlation	1	0.825	0.446	0.366	0.368	0.784	0.336	0.158	0.734
	P-value (2-tailed)		0.000	0.000	0.000	0.000	0.000	0.000	0.058	0.000
	N	144	144	141	142	144	144	141	144	72
Weight	Pearson's correlation	0.825	1	0.487	0.376	0.290	0.804	0.360	0.209	0.765
	P-value (2-tailed)	0.000		0.000	0.000	0.000	0.000	0.000	0.011	0.000
	N	144	148	145	145	148	148	145	148	74
LH	Pearson's correlation	0.446	0.487	1	0.296	0.129	0.553	0.196	0.094	0.473
	P-value (2-tailed)	0.000	0.000		0.000	0.121	0.000	0.020	0.258	0.000
	N	141	145	145	143	145	145	142	145	72
WHC	Pearson's correlation	0.366	0.376	0.296	1	0.146	0.337	-0.003	0.147	0.387
	P-value (2-tailed)	0.000	0.000	0.000		0.081	0.000	0.971	0.078	0.001
	N	142	145	143	145	145	145	142	145	72

WHS	**Pearson's correlation**	0.368	0.290	0.129	0.146	1	0.370	0.094	0.066	0.335
	P-value (2-tailed)	0.000	0.000	0.121	0.081		0.000	0.262	0.428	0.004
	N	144	148	145	145	148	148	145	148	74
PNS	**Pearson's correlation**	0.784	0.804	0.553	0.337	0.370	1	0.484	0.265	0.936
	P-value (2-tailed)	0.000	0.000	0.000	0.000	0.000		0.000	0.001	0.000
	N	144	148	145	145	148	148	145	148	74
IC	**Pearson's correlation**	0.336	0.360	0.196	-0.003	0.094	0.484	1	0.306	0.525
	P-value (2-tailed)	0.000	0.000	0.020	0.971	0.262	0.000		0.000	0.000
	N	141	145	142	142	145	145	145	145	73
IS	**Pearson's correlation**	0.158	0.209	0.094	0.147	0.066	0.265	0.306	1	0.206
	P-value (2-tailed)	0.058	0.011	0.258	0.078	0.428	0.001	0.000		0.079
	N	144	148	145	145	148	148	145	148	74
IHD	**Pearson's correlation**	0.734	0.765	0.473	0.387	0.335	0.936	0.525	0.206	1
	P-value (2-tailed)	0.000	0.000	0.000	0.001	0.004	0.000	0.000	0.079	
	N	72	74	72	72	74	74	73	74	74

A.5: Regression formula between PNS and height for combined measurements. The x represents the length of the neonate and the y represents the distance between the tip of the hamulus and the posterior nasal spine

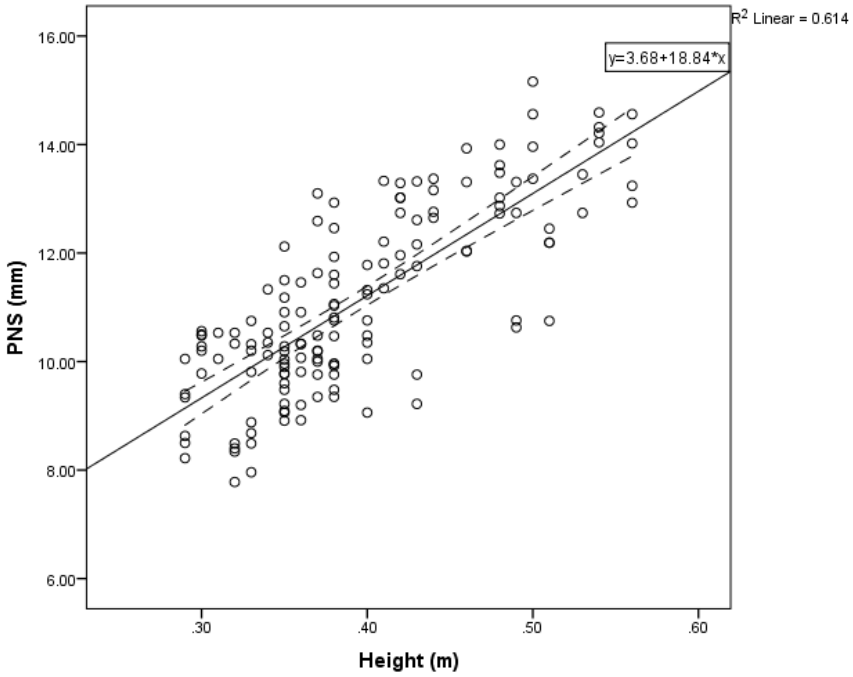

A.6: Regression formula between IHD and height for combined measurements. The x represents the height of the neonate and the y represents the distance between the two hamuli

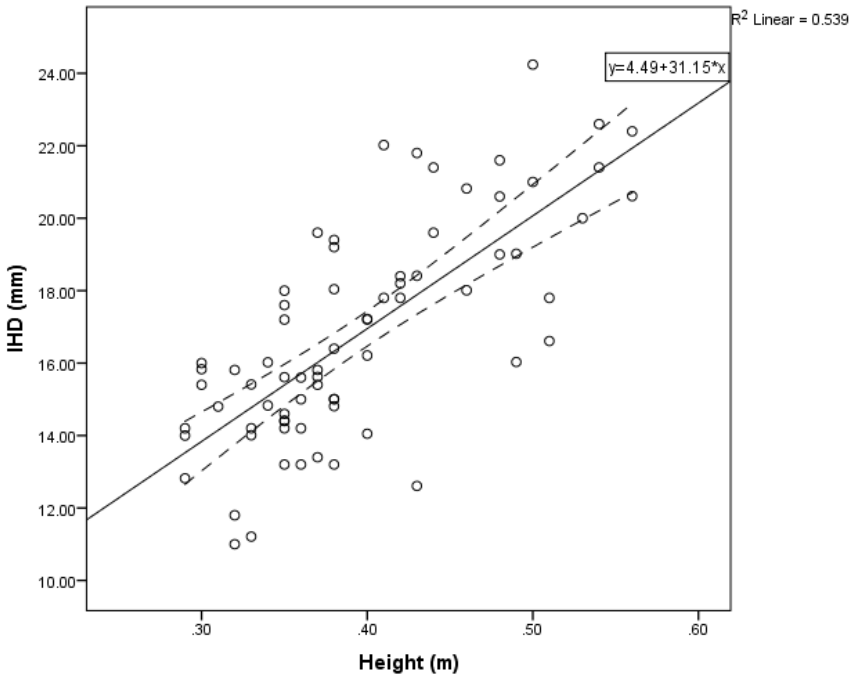

A.7: Regression formula between PNS and weight for combined measurements. The x represents the weight of the neonate and the y represent the distance from the hamulus to the posterior nasal spine

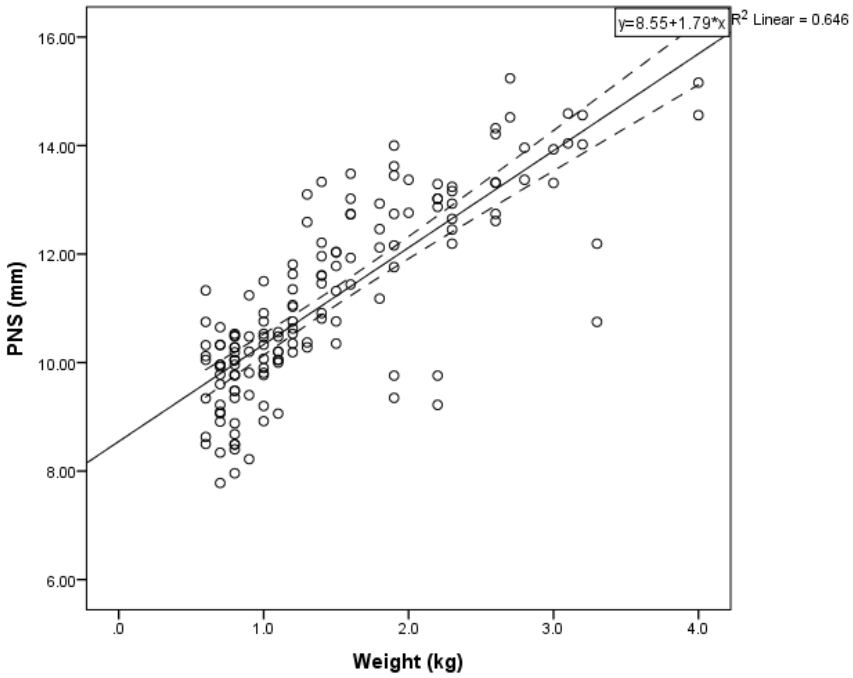

A.8: Regression formula between weight and IHD for combined measurements. The x represents the weight of the neonate and the y represents the distance between the two hamuli

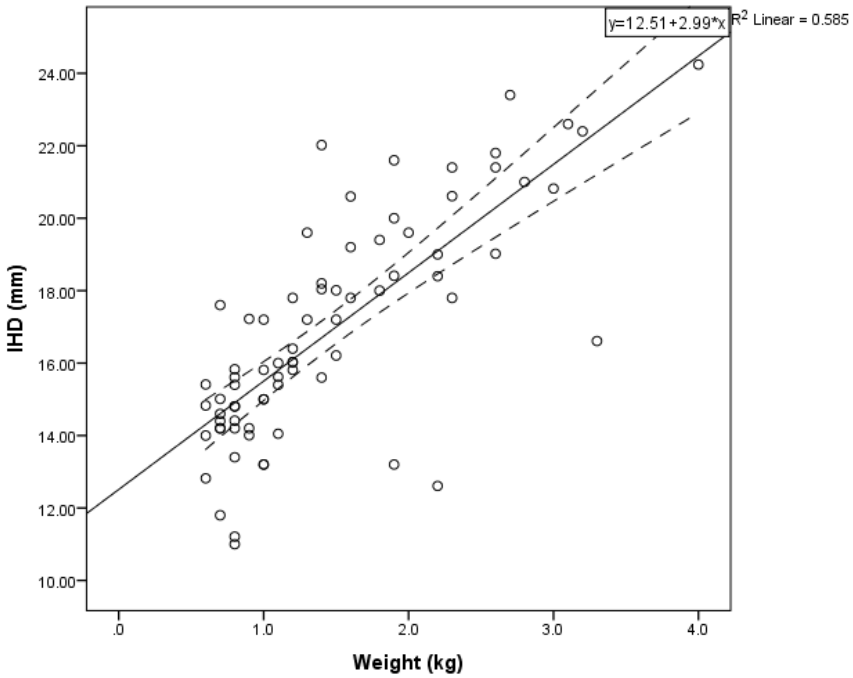

A.9: Regression formula between the IHD and the PNS for combined measurements. The x represents the distance between the two hamuli and the y represents the distance between the hamulus and the posterior nasal spine

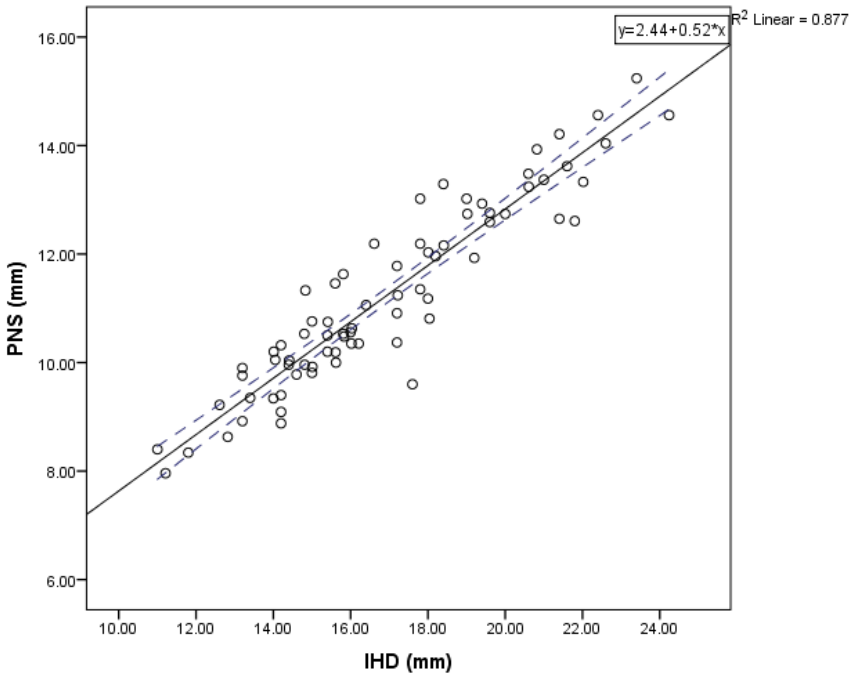

Appendix B

B.1: Pearson's correlation test indicating the strength of correlation between different measurements for W0. Green shows excellent correlation

		Height	Weight	LH	WHC	WHS	PNS	IC	IS	IHD
Height	**Pearson's correlation**	1	0.271	-0.141	0.171	-0.009	0.314	0.139	0.115	0.281
	P-value (2-tailed)		0.036	0.282	0.191	0.944	0.015	0.293	0.383	0.133
	N	60	60	60	60	60	60	59	60	30
Weight	**Pearson's correlation**	0.271	1	0.070	-0.112	0.073	0.194	-0.004	0.091	0.140
	P-value (2-tailed)	0.036		0.594	0.395	0.579	0.138	0.974	0.487	0.460
	N	60	60	60	60	60	60	59	60	30
LH	**Pearson's correlation**	-0.141	0.070	1	0.075	-0.040	0.436	-0.008	-0.095	0.404
	P-value (2-tailed)	0.282	0.594		0.569	0.763	0.001	0.950	0.469	0.027
	N	60	60	60	60	60	60	59	60	30
WHC	**Pearson's correlation**	0.171	-0.112	0.075	1	0.247	0.231	-0.160	0.278	-0.002
	P-value (2-tailed)	0.191	0.395	0.569		0.057	0.075	0.225	0.032	0.992
	N	60	60	60	60	60	60	59	60	30
WHS	**Pearson's correlation**	-0.009	0.073	-0.040	0.247	1	0.307	-0.045	0.247	0.346
	P-value (2-tailed)	0.944	0.579	0.763	0.057		0.017	0.732	0.057	0.061
	N	60	60	60	60	60	60	59	60	30
PNS	**Pearson's correlation**	0.314	0.194	0.436	0.231	0.307	1	0.143	0.067	0.773
	P-value (2-tailed)	0.015	0.138	0.001	0.075	0.017		0.281	0.612	0.000
	N	60	60	60	60	60	60	59	60	30
IC	**Pearson's correlation**	0.139	-0.004	-0.008	-0.160	-0.045	0.143	1	0.178	0.377
	P-value (2-tailed)	0.293	0.974	0.950	0.225	0.732	0.281		0.177	0.040
	N	59	59	59	59	59	59	59	59	30
IS	**Pearson's correlation**	0.115	0.091	-0.095	0.278	0.247	0.067	0.178	1	-0.008
	P-value (2-tailed)	0.383	0.487	0.469	0.032	0.057	0.612	0.177		0.965
	N	60	60	60	60	60	60	59	60	30
IHD	**Pearson's correlation**	0.281	0.140	0.404	-0.002	0.346	0.773	0.377	-0.008	1
	P-value (2-tailed)	0.133	0.460	0.027	0.992	0.061	0.000	0.040	0.965	
	N	30	30	30	30	30	30	30	30	30

B.2: Pearson's correlation test indicating the strength of correlation between different measurements for W1. Green shows excellent correlation, blue shows moderate correlation

		Height	Weight	LH	WHC	WHS	PNS	IC	IS	IHD
Height	**Pearson's correlation**	1	0.709	0.238	0.250	0.398	0.656	0.271	0.160	0.574
	P-value (2-tailed)		0.000	0.031	0.023	0.000	0.000	0.014	0.147	0.000
	N	84	84	82	82	84	84	82	84	42
Weight	**Pearson's correlation**	0.709	1	0.240	0.255	0.236	0.683	0.349	0.281	0.620
	P-value (2-tailed)	0.000		0.026	0.018	0.027	0.000	0.001	0.008	0.000
	N	84	88	86	85	88	88	86	88	44
LH	**Pearson's correlation**	0.238	0.240	1	0.251	0.028	0.286	0.128	0.127	0.114
	P-value (2-tailed)	0.031	0.026		0.022	0.798	0.008	0.247	0.246	0.468
	N	82	86	86	84	86	86	84	86	43
WHC	**Pearson's correlation**	0.250	0.255	0.251	1	0.0200	0.178	-0.084	0.146	0.335
	P-value (2-tailed)	0.023	0.018	0.022		0.856	0.104	0.448	0.182	0.030
	N	82	85	84	85	85	85	83	85	42
WHS	**Pearson's correlation**	0.398	0.236	0.028	0.020	1	0.368	0.155	-0.009	0.323
	P-value (2-tailed)	0.000	0.027	0.798	0.856		0.000	0.154	0.935	0.032
	N	84	88	86	85	88	88	86	88	44
PNS	**Pearson's correlation**	0.656	0.683	0.286	0.178	0.368	1	0.586	0.389	0.912
	P-value (2-tailed)	0.000	0.000	0.008	0.104	0.000		0.000	0.000	0.000
	N	84	88	86	85	88	88	86	88	44
IC	**Pearson's correlation**	0.271	0.349	0.128	-0.084	0.155	0.586	1	0.375	0.589
	P-value (2-tailed)	0.014	0001	0247	0.448	0.154	0.000		0.000	0.000
	N	82	86	84	83	86	86	86	86	43
IS	**Pearson's correlation**	0.160	0.281	0.127	0.146	-0.0090	0.389	0.375	1	0.331
	P-value (2-tailed)	0.147	0.008	0.246	0.182	0.935	0.000	0.000		0.028
	N	84	88	86	85	88	88	86	88	44
IHD	**Pearson's correlation**	0.574	0.620	0.114	0.335	0.323	0.912	0.589	0.331	1
	P-value (2-tailed)	0.000	0.000	0.468	0.030	0.032	0.000	0.000	0.28	
	N	42	44	43	42	44	44	43	44	44

B.3: Regression formula between the PNS and the IHD in the W0 sample. The x represents the distance from the hamulus to the posterior nasal spine. The y represents the distance between the two hamuli

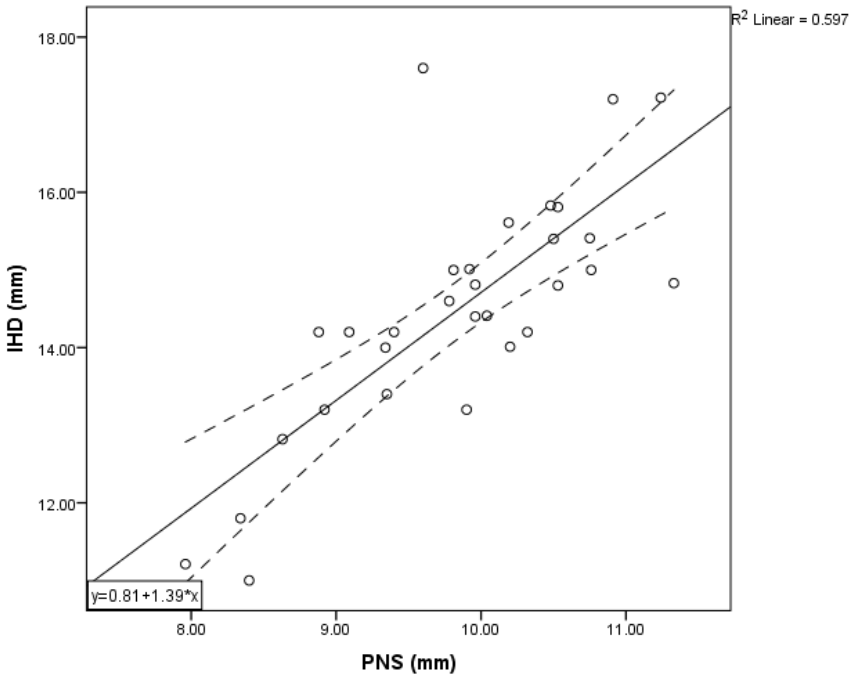

B.4: Regression formula between the PNS and the IHD in the W1 sample. The x represents the distance from the hamulus to the posterior nasal spine. The y represents the distance between the two hamuli

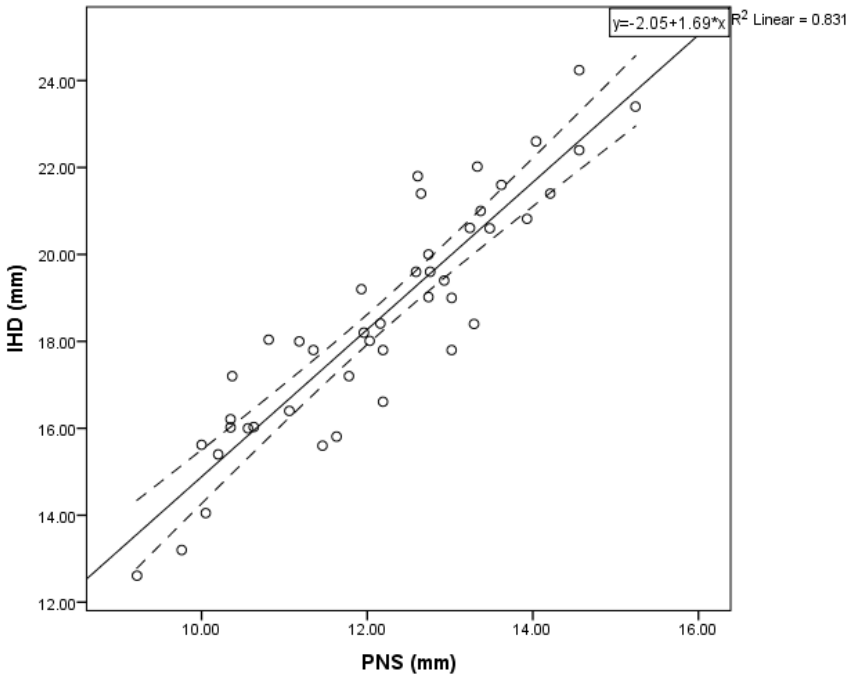

Appendix C

C.1: Pearson's correlation test indicating the strength of correlation between LH and the different measurements for the WA and BB populations. Green shows excellent correlation, blue shows moderate correlation

		Height	Weight	WHC	WHS	PNS	IC	IS	IHD
WA	Pearson's correlation	0.497	0.541	0.590	-0.017	0.708	0.347	0.292	0.682
	P-value (2-tailed)	0.003	0.001	0.000	0.924	0.000	0.041	0.084	0.002
	N	34	36	36	35	36	35	36	18
BB	Pearson's correlation	0.391	0.445	0.267	0.174	0.479	0.141	-0.019	0.394
	P-value (2-tailed)	0.000	0.000	0.005	0.069	0.000	0.147	0.844	0.003
	N	108	110	108	110	110	108	110	55

C.2: Regression formula between the LH and the PNS of the WA population. The x represents the length of the hamulus. The y represents the distance from the hamulus to the posterior nasal spine

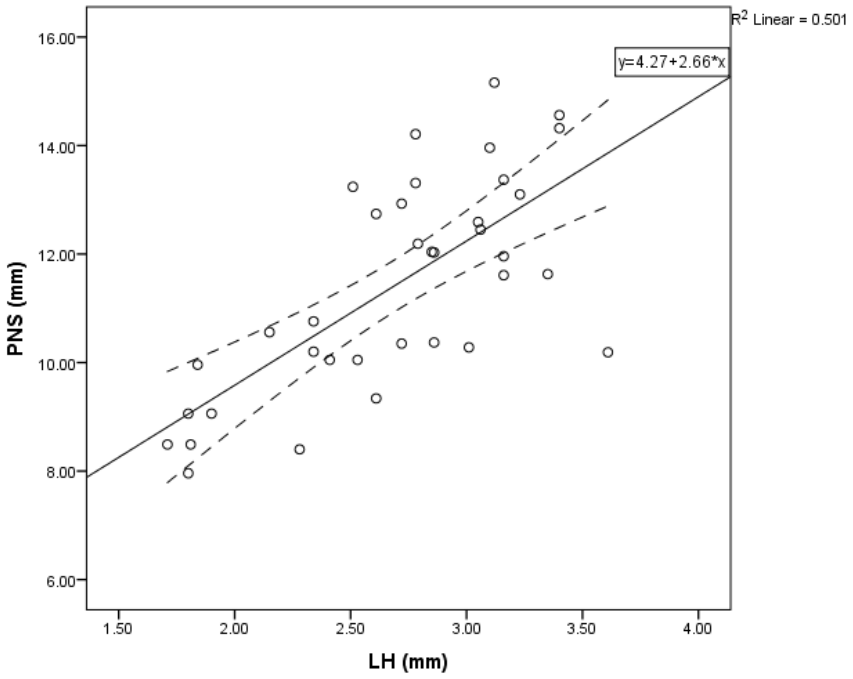

Appendix D

D.1: Visualisation of the Bland and Altman intra-observer error for LH (mm). The middle line shows the mean, with the dotted lines indicating the 95% CI and the most extreme lines indicate the upper and lower limit of repeatability

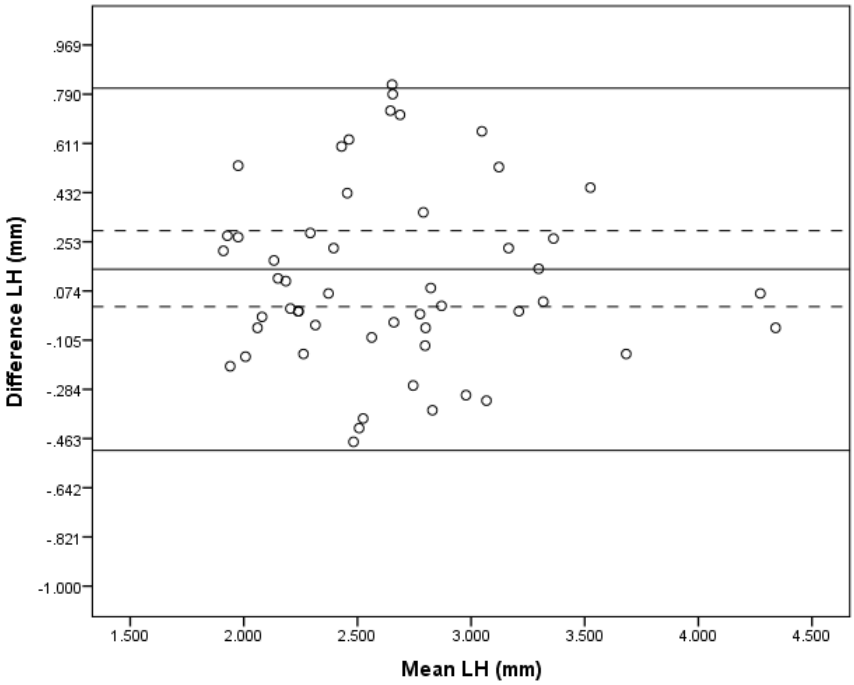

D.2: Visualisation of the Bland and Altman intra-observer error for WHC (mm). The middle line shows the mean, with the dotted lines indicating the 95% CI and the most extreme lines indicate the upper and lower limit of repeatability

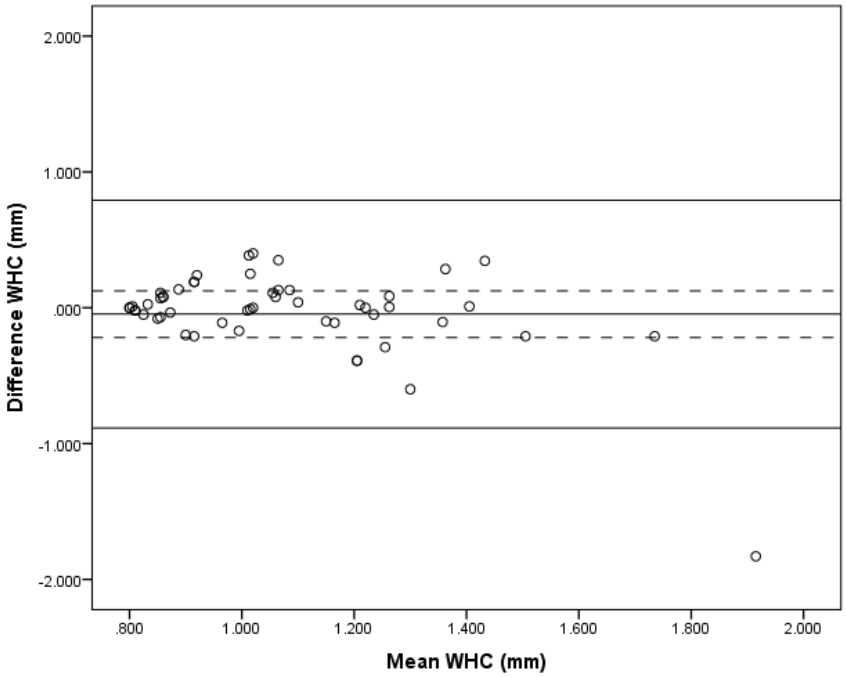

D.3: Visualisation of the Bland and Altman intra-observer error for WHS (mm). The middle line shows the mean, with the dotted lines indicating the 95% CI and the most extreme lines indicate the upper and lower limit of repeatability

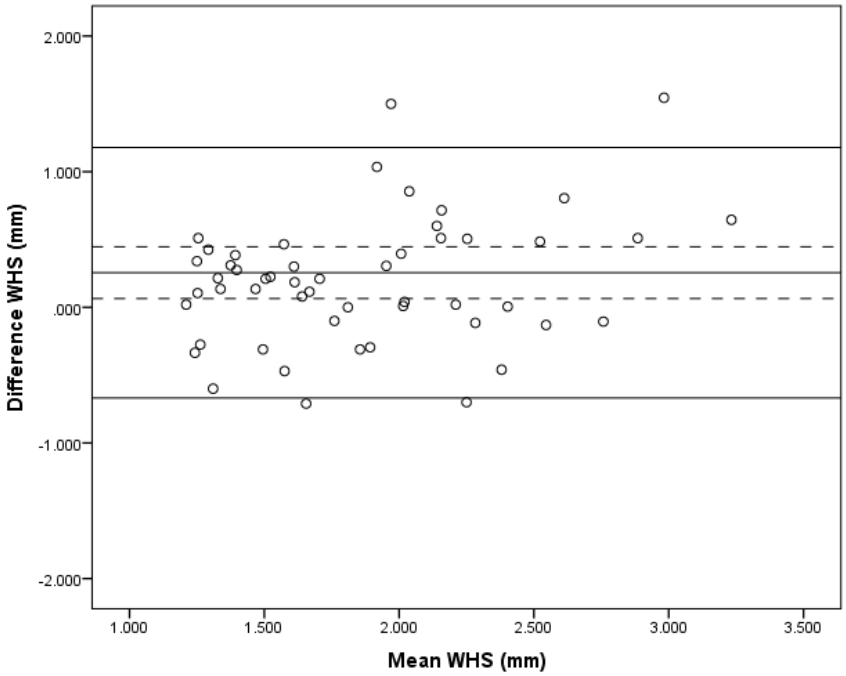

D.4: Visualisation of the Bland and Altman intra-observer error for PNS (mm). The middle line shows the mean, with the dotted lines indicating the 95% CI and the most extreme lines indicate the upper and lower limit of repeatability

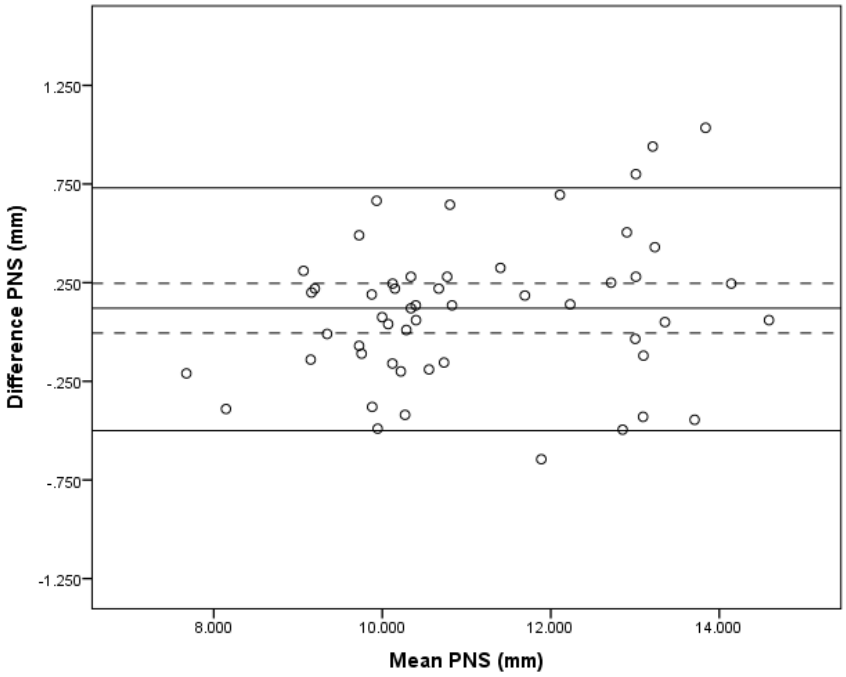

D.5: Visualisation of the Bland and Altman intra-observer error for IC (degrees). The middle line shows the mean, with the dotted lines indicating the 95% CI and the most extreme lines indicate the upper and lower limit of repeatability

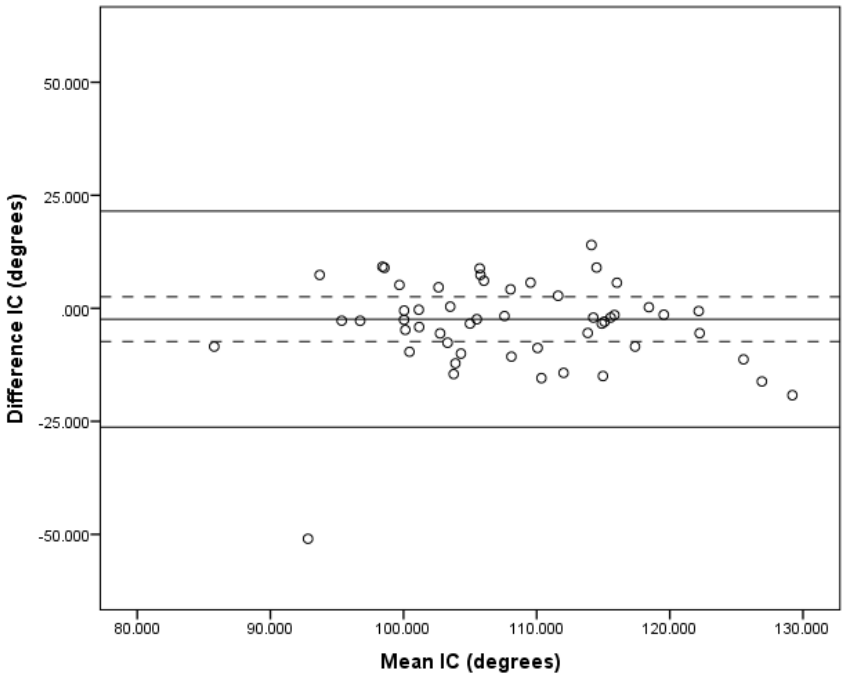

D.6: Visualisation of the Bland and Altman intra-observer error for IS (degrees). The middle line shows the mean, with the dotted lines indicating the 95% CI and the most extreme lines indicate the upper and lower limit of repeatability

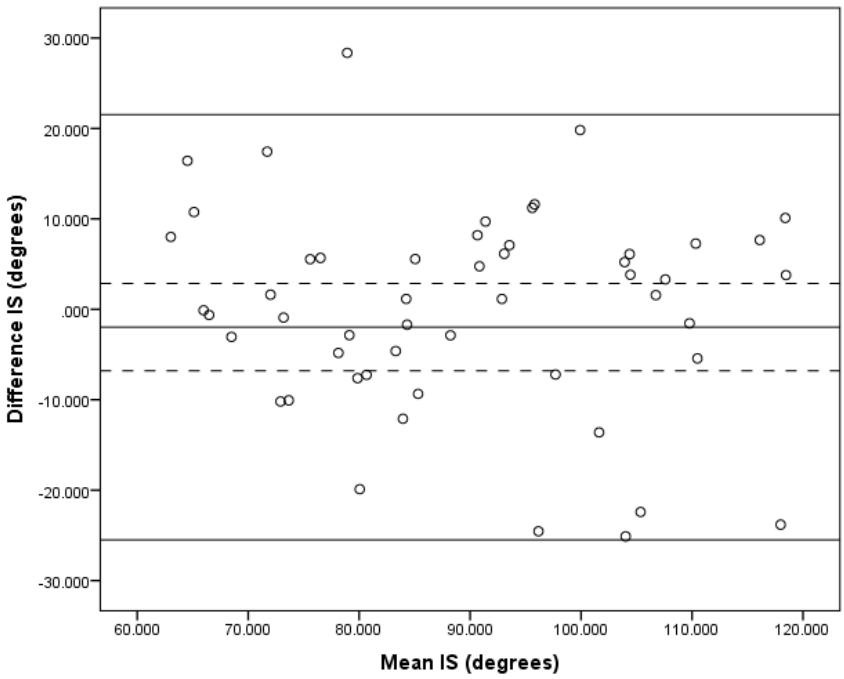

D.7: Visualisation of the Bland and Altman intra-observer error for IHD (mm). The middle line shows the mean, with the dotted lines indicating the 95% CI and the most extreme lines indicate the upper and lower limit of repeatability

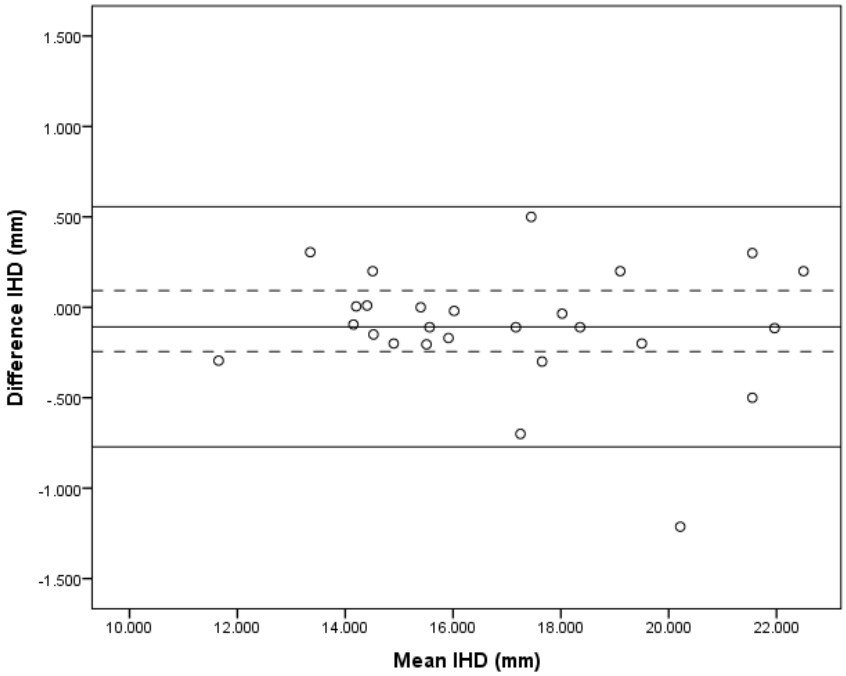

Appendix E

E.1: Visualisation of the Bland and Altman inter-observer error for LH (mm). The middle line shows the mean, with the dotted lines indicating the 95% CI and the most extreme lines indicate the upper and lower limit of agreement

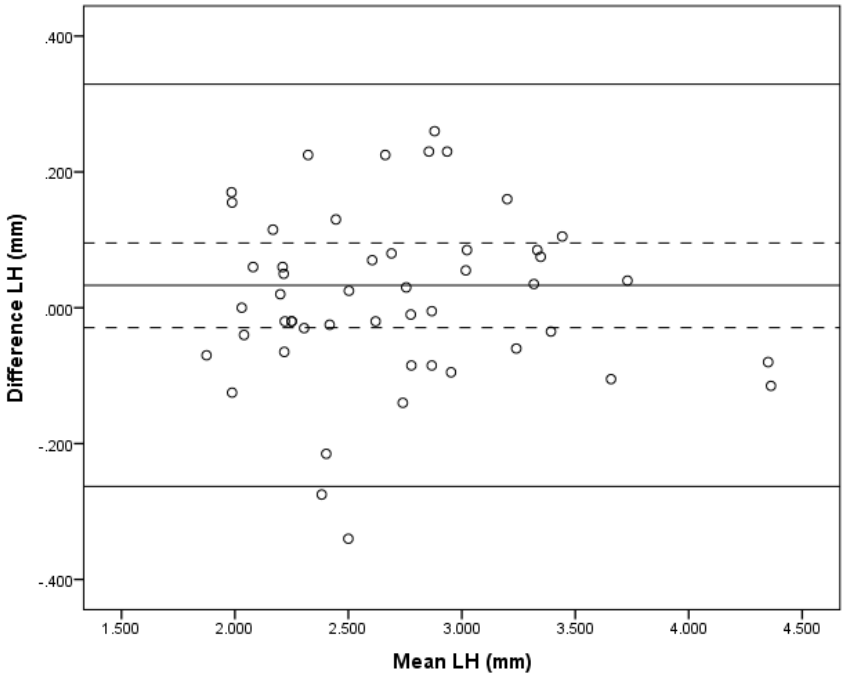

E.2: Visualisation of the Bland and Altman inter-observer error for WHC (mm). The middle line shows the mean, with the dotted lines indicating the 95% CI and the most extreme lines indicate the upper and lower limit of agreement

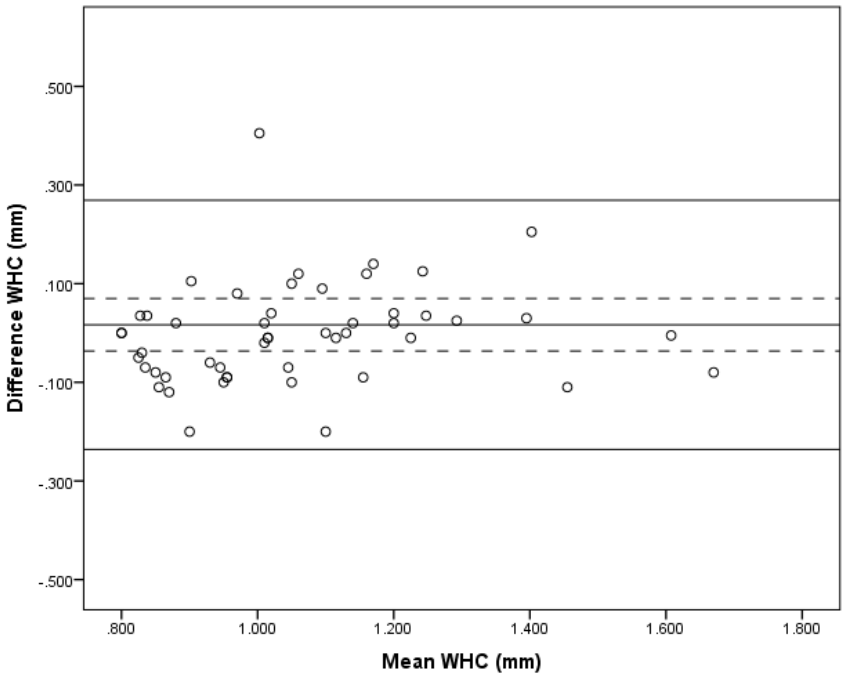

E.3: Visualisation of the Bland and Altman inter-observer error for PNS (mm). The middle line shows the mean, with the dotted lines indicating the 95% CI and the most extreme lines indicate the upper and lower limit of agreement

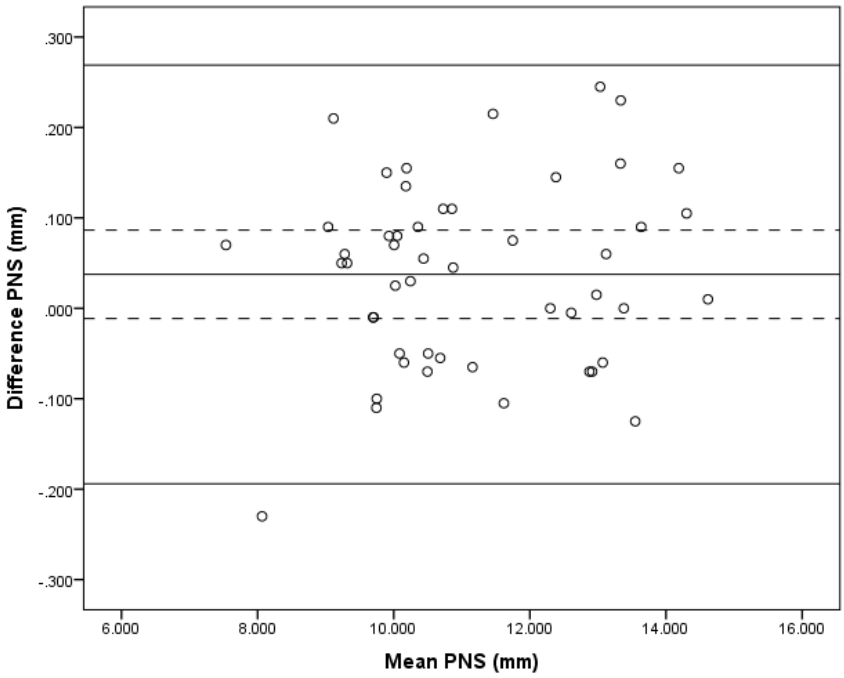

E.4: Visualisation of the Bland and Altman inter-observer error for IC (degrees). The middle line shows the mean, with the dotted lines indicating the 95% CI and the most extreme lines indicate the upper and lower limit of agreement

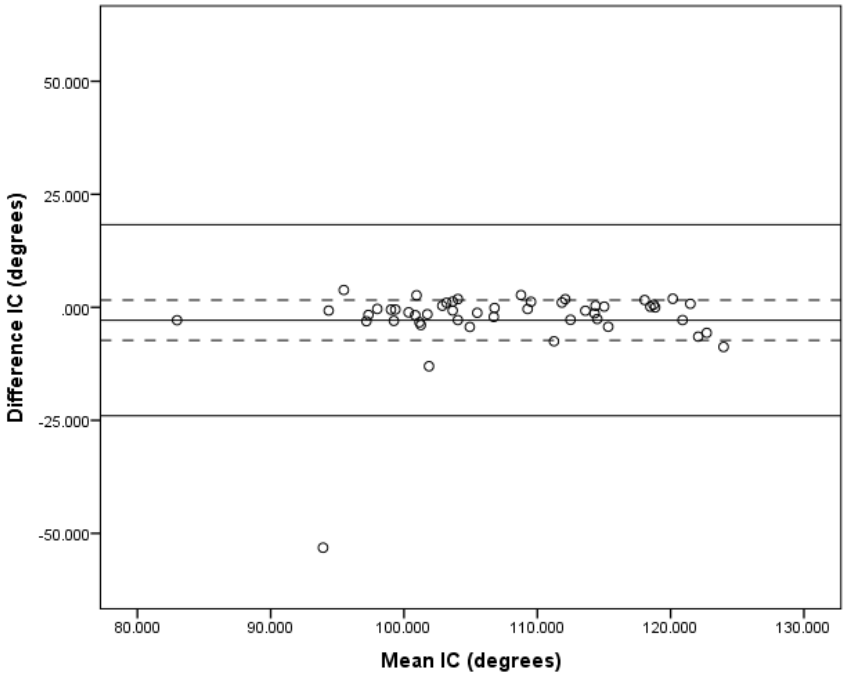

E.5: Visualisation of the Bland and Altman inter-observer error for SI (degrees). The middle line shows the mean, with the dotted lines indicating the 95% CI and the most extreme lines indicate the upper and lower limit of agreement

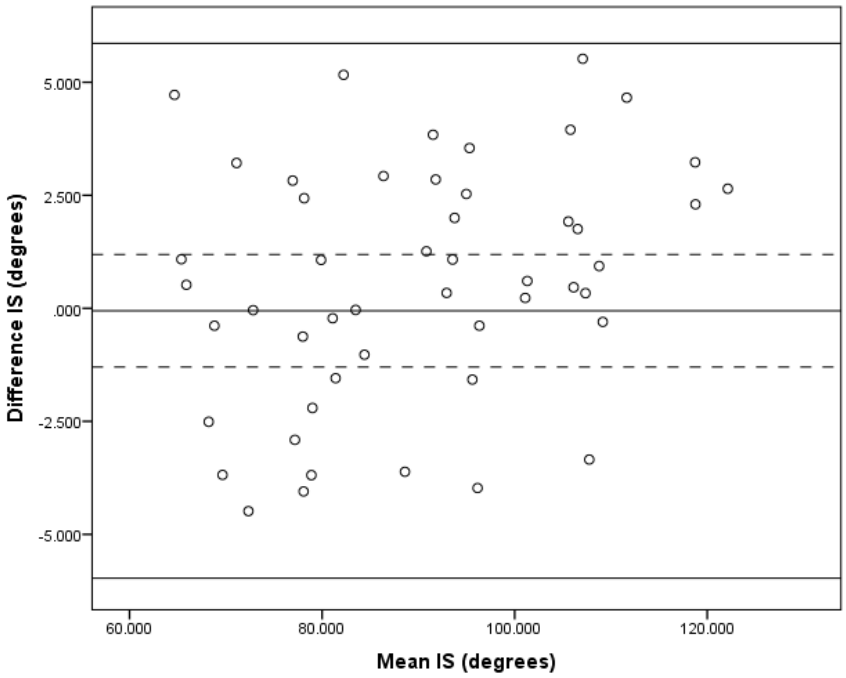

E.6: Visualisation of the Bland and Altman inter-observer error for IHD (mm). The middle line shows the mean, with the dotted lines indicating the 95% CI and the most extreme lines indicate the upper and lower limit of agreement

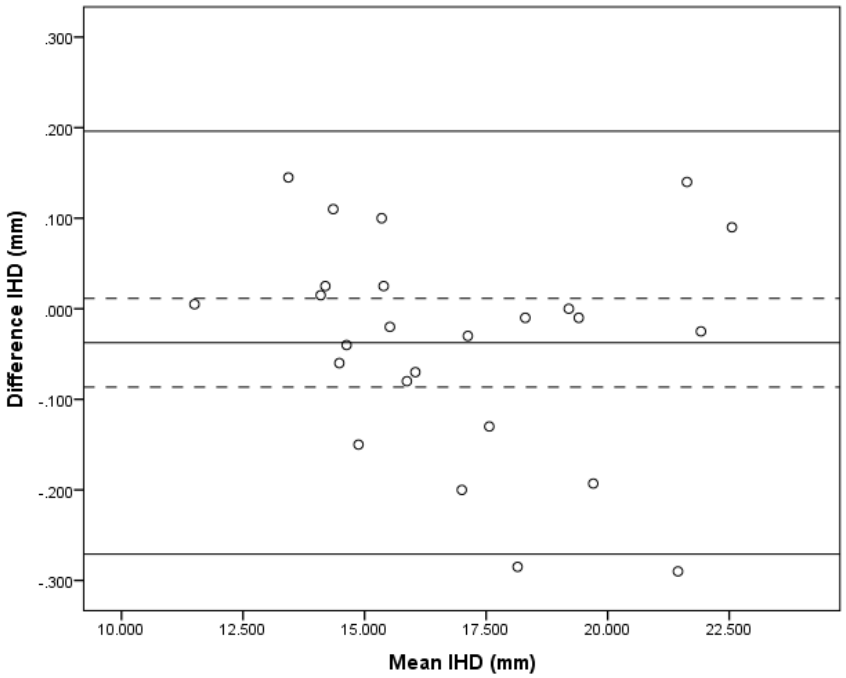

Appendix F

UNIVERSITEIT VAN PRETORIA
UNIVERSITY OF PRETORIA
YUNIBESITHI YA PRETORIA

Faculty of Health Sciences

The Research Ethics Committee, Faculty Health Sciences, University of Pretoria complies with ICH-GCP guidelines and has US Federal wide Assurance.

- FWA 00002567, Approved dd 22 May 2002 and Expires 03/20/2022.
- IRB 0000 2235 IORG0001762 Approved dd 22/04/2014 and Expires 03/14/2020.

10 October 2019

Approval Certificate
New Application

Ethics Reference No.: 667/2019
Title: Baseline morphometry of the pterygoid hamulus in a neonatal population

Dear Miss H Biemond

The **New Application** as supported by documents received between 2019-09-06 and 2019-10-09 for your research, was approved by the Faculty of Health Sciences Research Ethics Committee on its quorate meeting of 2019-10-09.

Please note the following about your ethics approval:

- Ethics Approval is valid for 1 year and needs to be renewed annually by 2020-10-10.
- Please remember to use your protocol number (667/2019) on any documents or correspondence with the Research Ethics Committee regarding your research.
- Please note that the Research Ethics Committee may ask further questions, seek additional information, require further modification, monitor the conduct of your research, or suspend or withdraw ethics approval.

Ethics approval is subject to the following:

- The ethics approval is conditional on the research being conducted as stipulated by the details of all documents submitted to the Committee. In the event that a further need arises to change who the investigators are, the methods or any other aspect, such changes must be submitted as an Amendment for approval by the Committee.

We wish you the best with your research.

Yours sincerely

Dr R Sommers
MBChB MMed (Int) MPharmMed PhD
Deputy Chairperson of the Faculty of Health Sciences Research Ethics Committee, University of Pretoria

The Faculty of Health Sciences Research Ethics Committee complies with the SA National Act 61 of 2003 as it pertains to health research and the United States Code of Federal Regulations Title 45 and 46. This committee abides by the ethical norms and principles for research, established by the Declaration of Helsinki, the South African Medical Research Council Guidelines as well as the Guidelines for Ethical Research: Principles Structures and Processes, Second Edition 2015 (Department of Health)

Research Ethics Committee
Room 4-60, Level 4, Tswelopele Building
University of Pretoria, Private Bag X323
Arcadia 0007, South Africa
Tel +27 (0)12 356 3084
Email deepeka.behari@up.ac.za
www.up.ac.za

Fakulteit Gesondheidswetenskappe
Lefapha la Disaense tša Maphelo